Dissertations   Theses and Dissertations

1968

The Radiopharmacological Evaluation of 75 Se-selenomethionine in Man

Moshe Ben-Porath
Loyola University Chicago

Recommended Citation

THE RADIOPHARMACOLOGICAL EVALUATION OF ^{75}Se-SELENOMETHIONINE

IN MAN

by

Moshe Ben-Porath

A Dissertation Submitted to the Faculty of the

Graduate School of Loyola University

in Partial Fulfillment of the

Requirements for the Degree

of Doctor of Philosophy

September, 1968

LIST OF FIGURES

LIST OF TABLES

LIST OF PUBLICATIONS THAT RESULTED FROM THIS DISSERTATION

1. M. Ben-Porath, G. Clayton, E. Kaplan: Selective Visualization of the Pancreas by Subtractive Double-radioisotope Scanning Technique. Transactions Amer. Nucl. Soc. 9:76-78, 1966.

2. E. Kaplan, M. Ben-Porath, S. Fink, G. Clayton, B. Jacobson: Elimination of Liver Interference from the Selenomethionine Pancreas Scan. J. Nucl. Med. 7:807-816, 1966.

3. E. Kaplan, M. Ben-Porath, S. Fink, G. Clayton, B. Jacobson: A Dual Channel Technique for Elimination of the Liver Image from Seleno-methionine Pancreas Organ Scans. In "Progress in Biomedical Engineering", L. J. Fogel and F. W. George (Ed.), pp 115-123, 1967.

4. M. Ben-Porath, G. Clayton and E. Kaplan: Energy-to-color Modulation for Multi-Isotope Scanning. Transactions Amer. Nucl. Soc. 10:80-82, 1967.

5. M. Ben-Porath, G. Clayton, E. Kaplan: Current Status of Multi-Isotope Scanning by Color Modulation (Abstract). J. Nucl. Med. 8:323, 1967.

6. E. Kaplan, M. Ben-Porath, S. Fink, G. Clayton, and B. Jacobson: Evaluation of Pancreatic Disease by Dual Color Scanning (Abstract). J. Nucl. Med. 8:349, 1967.

7. M. Ben-Porath, G. Clayton, E. Kaplan: Modification of a Multi-Isotope Color Scanner for Multi-Purpose Scanning. J. Nucl. Med. 8:411-425, 1967.

8. M. Ben-Porath, L. Case, E. Kaplan: The Biological Half Life of
^{75}Se-selenomethionine in Patients with Malignant Lymphomas (Abstract).
Fed. Proc. 27:668, 1968.

9. M. Ben-Porath, L. Case, E. Kaplan: The Biological Half Life of
^{75}Se-selenomethionine in Man. J. Nucl. Med. 9:168-169, 1968.

10. M. Ben-Porath, L. Case, E. Kaplan: Biological Half Life of
^{75}Se-selenomethionine in Man (Abstract). J. Nucl. Med. 9:303, 1968.

11. M. Ben-Porath, L. Case, E. Kaplan: The Use of a Tape Recorder in
Simultaneous Multi-Isotope Scanning (Abstract). J. Nucl. Med. 9:304,
1968.

12. E. Kaplan, S. Fink, M. Ben-Porath, G. Clayton: Diagnostic Efficacy
of Dual-Channel Pancreas Scanning (Abstract). J. Nucl. Med. 9:330,
1968.

13. S. Fink, M. Ben-Porath, B. Jacobson, G. Clayton and E. Kaplan:
Current Status of Dual Channel Pancreatic Scanning. J. Nucl. Med.
(in press).

14. M. Ben-Porath, G. Clayton, E. Kaplan: Evaluation of a Tape Recording
Device for Multi-Isotope Scanning (in press). J. Nucl. Med.

15. E. Kaplan and M. Ben-Porath: Clinical Application of Color Modulation
of Gamma Energy and Depth by Means of Dual Channel Scanning. In
"Proc. IAEA Symposium on Medical Radioisotope Scanning" (to be
published in January 1969).

16. E. Kaplan and M. Ben-Porath: Dual Isotope Scanning. In "The Medical
Clinics of North America" (to be published in spring 1969).

LIFE

MOSHE BEN-PORATH was born on January 7, 1932 in Czernowitz, USSR. He immigrated to Israel illegally (then Palestine) in 1947.

In 1948, during the War of Independence, he volunteered to the Israel Defense Forces, where he served as a sergeant of a demolition platoon till 1950.

He returned to high school after the war, and graduated in 1952. In the same year he enrolled in the Hebrew University of Jerusalem, majoring in Physics, with minors in Mathematics and Statistics. Through 1956/57, while serving as a graduate assistant in the department of Nuclear Physics, the author completed his masters thesis on "Gas Scintillators".

In 1957, he started to function as chief of the Medical Physics Section of the Hadassah University Hospital, Jerusalem. Throughout 1960 he was a research fellow in Medical Physics at the University of Texas Postgraduate School of Medicine in Houston. In 1961, he returned to his position in Jerusalem. Since 1965, the author is on leave of absence from his institution and a graduate student at the department of Pharmacology of Loyola University Stritch School of Medicine.

The author's research, to date, resulted in the publication of 30 articles and abstracts in the physical and biomedical literature.

ACKNOWLEDGMENT

CHAPTER I. INTRODUCTORY BACKGROUND

^{75}Se-selenomethionine and ^{75}Se-selenocystine were the first effective gamma-emitting label bearing amino acids analogs produced. Radioiodinated tyrosine was produced more than 10 years earlier, but was not usable for most studies, as its label is extremely cleavable in biological systems.

Since its synthesis in 1960, the biological properties of ^{75}Se-selenomethionine were extensively studied in animals. It has been clinically used for localization studies (scanning) of the pancreas, parathyroid and malignant lymph nodes. But little, if any, information was available on its fate in the human body. As a radioactive agent, the radiation dose delivered to the patient from a diagnostic procedure is of concern. One of the most important factors in calculating this dose is the biological half life of the compound. This factor in humans was estimated to be between 15 and 144 days. In addition, the radiation dose to various organs was calculated on the basis of distribution studies in animals.

The purpose of the present study, was the determination of the biological half life of ^{75}Se-selenomethionine in man. As there were reports of different localization patterns of the drug in healthy subjects, in patients with pancreatic diseases and in patients with malignant lymphomas, these three categories of subjects were chosen for the present studies. In addition, tissue distribution of ^{75}Se-selenomethionine was to be determined in man by in vivo counting and radioactive assay of

necropsy specimens.

In summary, the purpose of this study was:

1) Measurement of the biological half life of ^{75}Se-selenomethionine in man.

2) Comparison of the fate of ^{75}Se-selenomethionine in healthy subjects, patients with pancreatic disease and with malignant lymphomas.

3) Determination of the tissue distribution of ^{75}Se-selenomethionine in man.

4) Calculation of the radiation dose from ^{75}Se-selenomethionine to the whole body and specific organs in man.

5) The investigation of the possible uses of ^{75}Se-selenomethionine in Nuclear Medicine and the design of suitable instrumentation for this purpose.

I-a. ^{75}Selenium$_{34}$.

Kent and Cork, in 1942, were the first to produce and identify the radionuclide ^{75}Selenium$_{34}$ by the bombardment of ^{75}As$_{33}$ with deuterium (1). Hopkins described it as decaying by K-capture with a half life of 120 days (2).

Cork and associates were the first to determine the energy levels associated with ^{75}Se-selenomethionine by spectrometry (3). Jensen and associates determined the relative weight of the various transitions in the decay scheme, using 180° spectrometry and pulse height analysis (4). These results were confirmed by Schardt and Welker (5). Fig. 1 shows

Figure 1. The decay scheme of $^{75}Se_{34}$ (6)
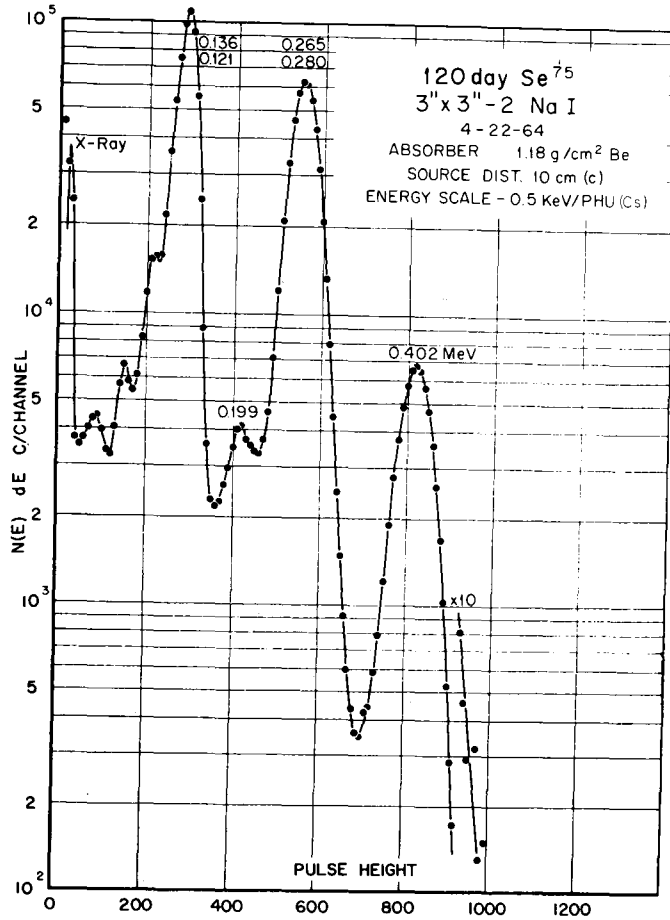
Figure 2. Pulse-height analysis spectrum of $^{75}Se_{34}$
(0.265-0.280 kev peaks counted in Nuclear Medicine applications)

the decay scheme of $^{75}Se_{34}$ as summarized by Dzhelepov and Peker (6). A pulse height analysis spectrum is shown in fig. 2.

$^{75}Se_{34}$ is produced today in the reactor by the following nuclear reaction:

$$^{74}Se_{34} + {^1n_o} \longrightarrow {^{75}Se_{34}} + \gamma$$

The cross section of this reaction is 0.23 barns, indicating that a 5g ^{75}Se-selenomethionine target left in the reactor for one week exposed to a neutron flux of $10^{12}n/cm^2/sec$ will yield 8 mCi ^{75}Se-selenomethionine (7).

I-b. ^{75}Se-selenomethionine.

I-b-1. Synthesis. ^{75}Se-selenomethionine is a seleneated radioactive analogue of the natural occurring amino acid methionine. The structure of the two compounds are shown in fig. 3. It was first prepared in a racemic form by Painter (8), but because of the complicity of the method it was not used. In 1960 Blau prepared ^{75}Se-selenomethionine by the following method: Baker's yeast (Saccharomyces cerevisiae) was grown on the low-sulfur containing media of Williams and Dawson, containing per liter: glucose, 20 g; $(NH_4)_2HPO_4$, 3.5g; KH_2PO_4, 0.2g; $MgSO_4 \cdot 7H_2O$, 0.25g; sodium citrate, 1.0g; L-asparagine monohydrate, 2.5g; biotin, 10g; calcium pantothehate, 0.5 mg; inositol, 10 mg; thiamine, 6 mg; pyridoxine, 1 mg; Zn^{2+} (as acetate), 400 g; Fe^{3+} (as chloride) 150 g; Cu^{2+} (as chloride), 25 g $\cdot$ $H_2{}^{75}SeO_3$ (ORNL Se-75-P-2 processed, enriched) was added and the medium adjusted to pH 5 with H_3PO_4. Up to 10 mC/l of ^{75}Se-selenomethionine

$$CH_3-S-CH_2-CH_2-\underset{\underset{\displaystyle NH_2}{|}}{CH}-COOH$$

METHIONINE

$$CH_3-Se-CH_2-CH_2-\underset{\underset{\displaystyle NH_2}{|}}{CH}-COOH$$
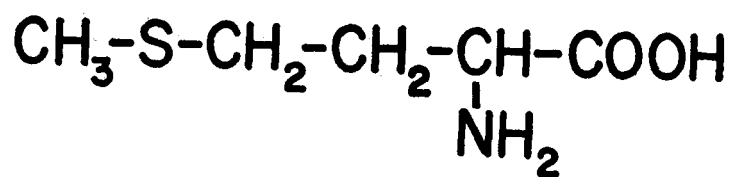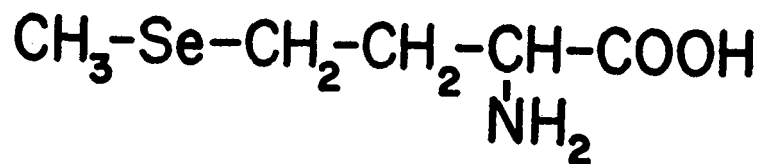
SELENOMETHIONINE

Figure 3. Structures of methionine and selenomethionine

has been used without noticeable decrease in the growth rate of the yeast. After inoculation with 50 mg of pressed yeast, growth was carried out in 3-1 Fernbach flasks containing 500 ml of media. Vigorous agitation provides aeration and the temperature was maintained at approximately 30°. Growth and subsequent chemical manipulation were carried out in fume hood to prevent inhalation of volatile selenium compounds.

The yeast was harvested by centrifugation after 18-24 h. Inoculation of ^{75}Se-selenomethionine into cells proceeds to approximately 50% and then stops. This yield can be increased by adding glucose to the media after the first harvest readjustment to pH 5 and allowing growth to proceed for another 24 h. An additional 25% yield was obtained.

The yeast was dehydrated with ethanol and refluxed 30 min. with ligroin to remove lipid material. After washing with ethyl ether the yeast was air dried. To remove carbohydrates, the dry yeast (1-3g) was extracted with 70 ml 5% trichloroacetic acid for 15 min. at 90° and washed once with cold trichloroacetic acid. 75-80% of the yeast radioactivity remained in the insoluble protein fraction. 100 mg each of L-methionine and L-cystine were added and the yeast protein was hydrolyzed 5 h. in boiling 5 N HCL. Bumping was controlled with glass wool. Control of bumping by vigorous shaking or bubbling with air reduced the yield. Immediately after hydrolysis the humin was centrifuged or filtered off and the HCl removed by vacuum evaporation to dryness 3-5 times. The residue was taken up in 200 ml water. The pH at this point must be over 1.5. This solution contains 50-60% of the original yeast radioactivity.

The selenium amino acids were separated by ion-exchange chromatography

on Dowex-50-X8 resin. 200-400 mesh resin, cleared of fines by repeated

decantation, was prepared in a column 1 in. in diameter and 5 in. long.

The resin was pretreated on the column with 4N HCL and then washed until

the pH of the effluent is over 2.

The protein hydrolysate was passed through the column at 2-3 ml/min

followed by 150-200 ml of wash water. 95-98% of the radioactivity remains

on the column. ^{75}Se-selenomethionine was eluted with 1.1 N HCL passed

through the column at the rate of 1.5-2.0 ml/min. Radioactivity in the

effluent was followed by counting one-drop samples taken every 10 ml.

^{75}Se-selenomethionine appeared in the eluate between 300-500 ml, resembling

quite closely the elution of (^{35}S) methionine from this resin.

The yield by this method was about 25% of the initial radioactivity.

I-b-2. Distribution, fate and excretion. Thirty minutes following

an intravenous injection of ^{75}Se-selenomethionine, the blood level drops to

20% of its two minute level. Then it gradually rises up to 75% at 4 hours

when it reaches plateau and slowly declines to 60% at 24 hours (11).

Penner showed that practically all the ^{75}Se-selenomethionine activity

reappearing in the blood is incorporated in serum proteins (12). In his

experiment the peak and plateau were reached at 5 hours, and accounted

for 25% of the administered dose.

Awad found the maximum protein bound activity at 8 hours, accounting

for 22% of the administered dose (13). He also showed that the biological

half life of the plasma proteins was 17 days, the main fraction being in

albumin (half life 8 days). Penner found that the incorporation into

erythrocytes is considerably less than in plasma, and that at least 85% of the RBC ^{75}Se-selenomethionine was incorporated in hemoglobin (14). Awad confirmed this result, but studying the aspect of RBC ^{75}Se-selenomethionine activity more extensively reported that the maximum concentration in RBC occurs at 35 days (5% of injected dose), when it reaches a plateau up to 100 days, then a decline starts reaching minimal levels at 135 days (13). He suggested that this pattern follows very much the life span of the erythrocyte. He accounted for 95% of the ^{75}Se-selenomethionine in the RBC as being incorporated in hemoglobin.

These results were recently confirmed (15).

Many laboratories studied the tissue distribution of ^{75}Se-selenomethionine in various species, at various times following an intravenous injection.

Blau and Manske reported the relative specific activity in dogs, 2 hours after the injection to be (10):

Pancreas : Liver : Spleen : Kidney : Blood = 30 : 6 : 1 : 5 : 1.5

Zuidema and Kirsh (16) found in the monkey, that 2 hours after injection a ratio of:

Pancreas : Liver : Kidney = 3.5 : 2.5 : 1

Anguileri and Marques found 8 hours and 7 days after injection the following ratios in the mouse (17):

8 hours : Pancreas : Liver : Kidney : Testis = 4.5 : 1.7 : 4.2 : 1

7 days : Pancreas : Liver : Kidney : Testis = 0.6 : 0.7 : 1.1 : 1

They found over a period of 7 days that while the pancreas activity disappears fast, the testicular and skeletal muscle activity increase slowly, and a slow disappearance in all other organs. Awad and co-workers compared the distribution in rats at 30 minutes and 24 hours after the administration (18):

30 minutes : Pancreas : Liver : Kidney : Muscle = 15 : 6 : 6 : 1

24 hours : Pancreas : Liver : Kidney : Muscle = 5 : 4 : 6 : 1

They found that while at 30 minutes between 60% and 77% of the ^{75}Se-seleno-methionine was incorporated in proteins in the various tissues investigated, at 24 hours more than 95% was incorporated.

Sternberg and Imbach studied the distribution of ^{75}Se-selenomethionine on the subcellular level in the rat liver cells and found 60 minutes after the injection (19):

Microsomes	17.8%
Mitochondria	11.8%
Nucleus	10.9%
Supernatant	50.4%
TCA precipitate	9.1%

Awad and co-workers reported that after degradation of ^{75}Se-seleno-methionine, ^{75}Se may reappear in the precursor amino acid pool of the liver in forms of L-^{75}Se-selenocystine and L-^{75}Se-selenocysteine.

^{75}Se-selenomethionine is excreted in the urine (15,21,22) bile (15) and by expiration (19). The rate of excretion varies widely from species to species. It has been reported that 80% was excreted in 12 weeks in dogs,

"while in monkeys the excretion is considerably slower" (15). In mice it was found to be 7 days (17). In rats 15-20 days (23). Attempts have been made by various investigators to estimate biological half life of ^{75}Se-selenomethionine in man on the basis of animal data. The results vary from 15-20 days (23,24), to 23 days (21,26,27,28), to 100 days (22,24,25) and up to 144 days (30). According to these figures, the respective investigators have calculated the whole body irradiation delivered by a tracer dose of 250 µci ^{75}Se-selenomethionine anywhere between 0.6 rads (23) to 2.3 rads (30).

I-b-3. Amino acid properties of ^{75}Se-selenomethionine. The biological behaviour of ^{75}Se-selenomethionine has been compared to that of ^{35}S-methionine and natural occurring L-methionine. Its incorporation into proteins and the fate of ^{75}Se-selenomethionine containing proteins have been compared to ^{35}S-methionine analogue compounds (31-37).

Spencer and Blau (31) studied the intestinal transport of ^{75}Se-selenomethionine in the hamster. By administering simultaneously the ^{75}Se-selenomethionine and ^{35}S analogues, they found identical transport across the everted hamster intestine sacs in the presence of carrier methionine. They found the k_m for both amino acids to be 0.8 X 10^{-3}M, suggesting the compound to be a good indicator for amino acid absorption studies. Hansson and Blau (32) reported identical rate and amount of incorporation of ^{75}Se-selenomethionine and natural L-methionine in pancreatic juice in the cat.

Autoradiographic studies performed by Hansson and Jacobsson in the mouse, as well as in vitro counts of tissue homogenates seem to indicate that the incorporation of ^{75}Se-selenomethionine and the natural amino acid into proteins follow the same pathway (34). Ochoa and Gitler (36) injected ^{75}Se-selenomethionine into the chicken wing and showed incorporation into the egg white protein. They found that it is incorporated in a manner indistinguishable from natural L-methionine. They suggest that it is bound to the protein by a strong covalent bound as it is not removable by dialysis, gel filtration or TCA precipitation. In another experiment (37) they showed that the digestion, absorption, ingestion and secretion of ovalbumin labelled with ^{75}Se-selenomethionine is identical to that labelled with ^{35}S-methionine. However, Holland and co-workers (33,35) showed, that in some instances ^{35}S-methionine and ^{75}Se-selenomethionine behave differently. They found that under some specific dietary conditions the total body disappearance of ^{75}Se-selenomethionine after feeding is significantly faster than that of ^{35}S-methionine given simultaneously. They concluded that ^{75}Se-selenomethionine is in a metabolic pool separate from methionine. In another experiment they fed mice radioactive diets containing both ^{75}Se-selenomethionine and ^{35}S-methionine at a 1:1 ratio. Over a period of time the total mouse ratio of ^{75}Se:^{35}S was 1.46, and in Krebs-2 tumor bearing mice the ratio in the tumor was 3.60.

In conclusion, most of the evidence in the literature seems to indicate that ^{75}Se-selenomethionine, ^{35}S-methionine and natural methionine behave biologically in a similar manner. Differences were observed under special dietary conditions.

I-c. Medical applications of ^{75}Se-selenomethionine.

I-c-1. Pancreatic scanning. The use of ^{75}Se-selenomethionine for the scanning of the pancreas was first suggested by Blau and Manski (10) from data obtained on dogs. In 1962 Blau and Bender reported the first successful pancreatic scans in man (29). However, the close anatomic relationship of the pancreas and the liver presented a serious problem. Although the ^{75}Se-selenomethionine concentration in liver tissue is less than in the pancreas (1:5), the total activity in the liver is much greater due to its more than 20 fold larger mass. Therefore, the visualization of the pancreas was obstructed in most by strong γ-emission from the adjacent liver (10,21-30,40-53). Thus, various methods have been suggested to improve the visualization of the pancreas. Sodee suggested the blocking of the estimated liver area with heavy lead shields (26,28). Rodriguez-Antunez suggested the administration of $\frac{1}{4}$ grain morphine 30 minutes before the ^{75}Se-selenomethionine to induce constriction of the sphincter of Oddi, slowing the secretion of pancreatic juice and allowing for a higher build-up of radioactivity in the pancreas (43,44). Tabern claimed to improve the visualization of the pancreas by administering the ^{75}Se-selenomethionine 15 minutes after an intravenous infusion of an amino acid mixture for enzyme synthesis which was continued throughout the scanning procedure (50). Other methods required the overnight fasting of the patient, 2 glasses of milk for breakfast, 3 hours later 1 unit per kg body weight pancreozymin, to empty the pancreas and stimulate fresh enzyme synthesis. After another hour the ^{75}Se-selenomethionine was given I.V., plus 15 mg oral Probanthine to inhibit
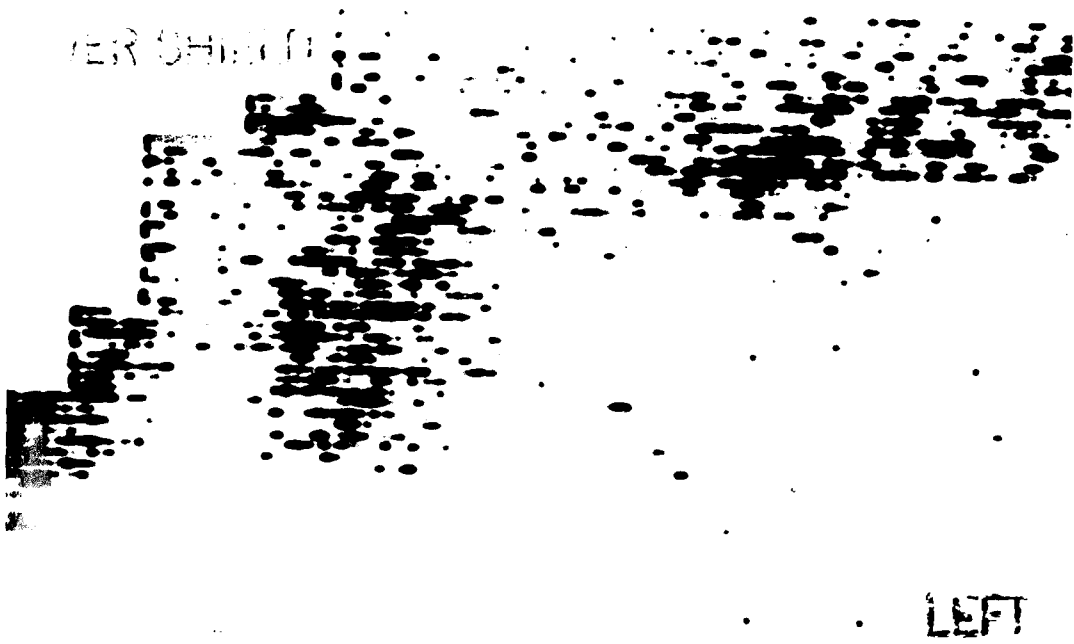
Figure 4.   Pancreatic scan - lead shield (26)
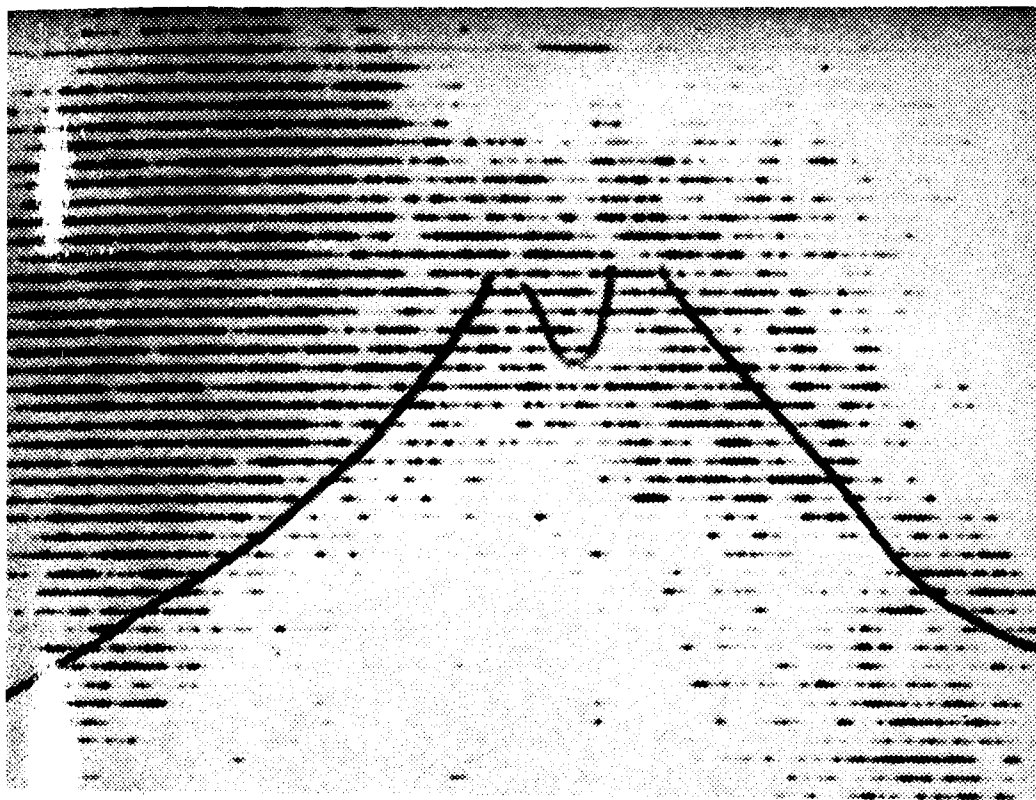
Figure 5. Pancreatic scan - morphine (44)
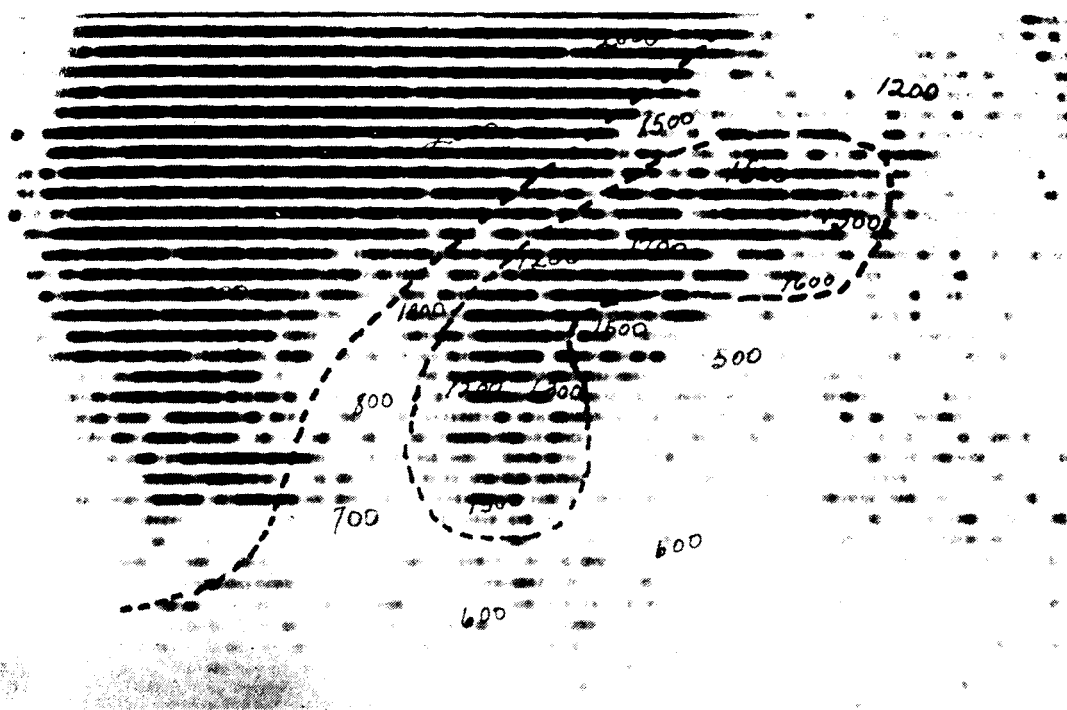
Figure 6. Pancreatic scan - amino acid mixture (50)
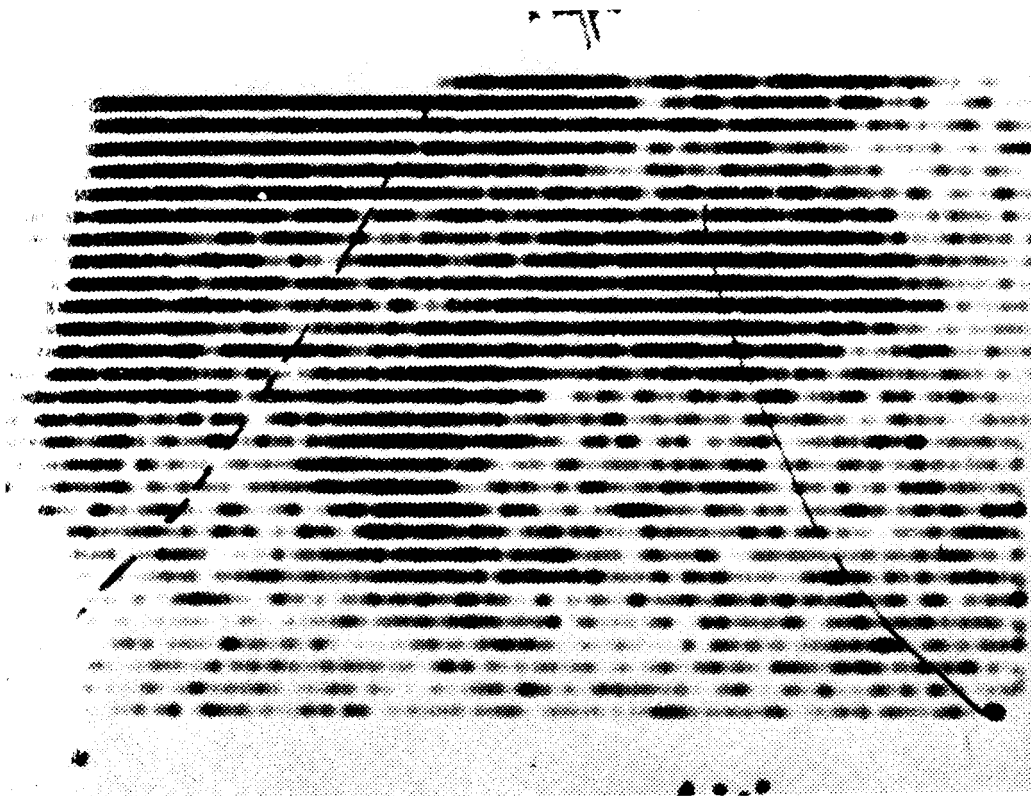
Figure 7. Pancreatic scan - milk breakfast (38)

pancreatic secretion. The scanning was to be started 30 minutes later

(29,46). High protein breakfast and 900 mg orally administered glutamic

acid to stimulate pancreatic enzyme synthesis have also been employed (26,

28, 53). Replacement of the high protein breakfast by an I.V. administration

of 35 g. glucose 30 minutes prior to the ^{75}Se-selenomethionine injection was

suggested (52). All workers agree that 3 μCi/kg ^{75}Se-selenomethionine is

an adequate dose for this procedure. This has been standardized to 250

μCi total dose, except in cases of extreme weights.

With all the techniques employed, the procedure of pancreatic scanning

remained unsatisfactory, principally because of the liver interference, and

was not widely used clinically. Figures 4, 5, 6 and 7 are examples of the

best published scans produced by the above described techniques. It is

evident, that unless there is a complete anatomical separation between the

liver and the pancreas, the visualization of the latter is unsatisfactory.

I-c-2. Parathyroid scanning. In 1963, Potchen demonstrated the

concentration of tritiated methionine in the rat parathyroid (64). In

1964, DiGiulio and Beierwalters gave 250 μCi ^{75}Se-selenomethionine to

patients scheduled for surgery due to suspected parathyroid adenoma.

They showed a 2.5:1.0 ratio of parathyroid to thyroid tissue specific

concentrations (21,27). But due to the adjacency of these two organs

and the larger mass of the thyroid, the outline of the parathyroid on

the scan is largely masked, and its visualization extremely difficult.

While some workers claim to be able to visualize adenoma of the para-

thyroid and hyperactive glands, their published results (figs. 8 and 9)

PARATHYROID SCAN
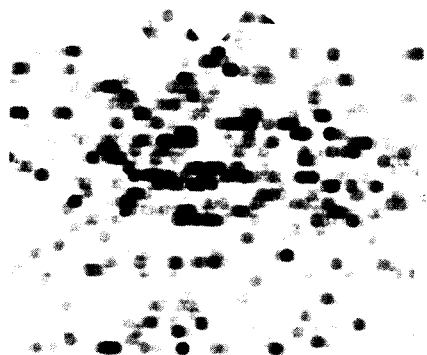
L.C. #148116

250 μc Se^{75}
        Methionine

Time: 8 hr.

Date: 8/23

⟵———— Supra Sternal Notch

Figure 8. Parathyroid scan (55)
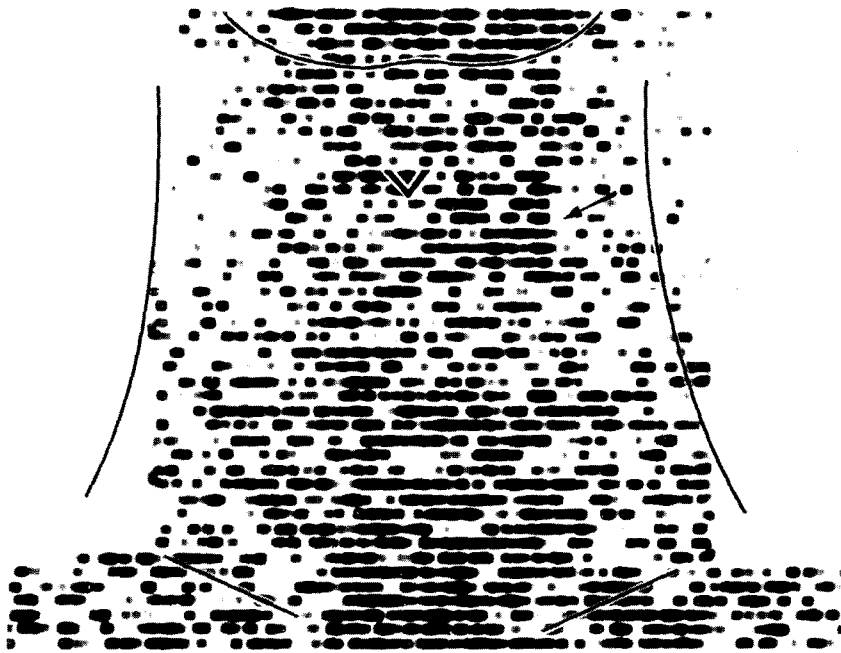
Figure 9. Parathyroid scan (60)

do not support this claim (54-58,60). Gottschalk sought to improve the visualization of the parathyroid by bilateral intra-arterial administration of the agent in the thyrocervical trunk (59). Marshall reported that while scanning attempts were unsuccessful, ultrastructural changes were observed in malignancy of the parathyroids in patients who received 100-200 μCi ^{75}Se-selenomethionine. No such changes were observed in patients that did not receive the drug (61).

I-c-3. Scanning malignant lymphomas. While performing a pancreatic scan in a patient with jaundice, Herrera observed on the photoscan a large abdominal mass that concentrated ^{75}Se-selénomethionine. This lesion was proven to be lymphosarcoma by needle biopsy, and later by autopsy (62). They studied 10 additional patients with malignant lymphomas (7 lymphosarcoma, 2 Hodgkin's disease, 1 Reticulum cell sarcoma) and obtained 7 positive scans. No false positives were observed in a control group containing 6 patients with malignant and benign diseases of none lymphatic origin. Following this observation, Spencer obtained positive scans in 19 out of 35 patients with malignant lymphomas (63). Figure 10 is an example of a positive scan. In an experiment on L5178Y lymphoma cell injected mice, he showed that the relative concentration of ^{75}Se-selenomethionine in Liver : Tumor : Muscle was 16 : 5 : 1.

Attempts to use ^{75}Se-selenomethionine for thyroid studies (51) and liver scanning (39) were unsuccessful.

Shimazu and Tappel reported in 1964 that selenoamino acids have
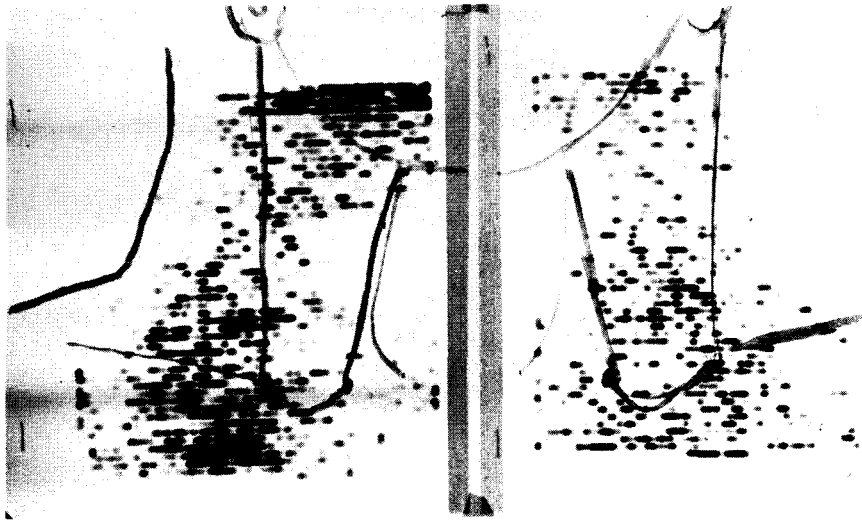
Figure 10. Lymphoma scan (62)

radioprotective properties (65,66). This interesting property, however, has so far received little treatment in the literature.

I-d. <u>In Vivo counting</u>.

I-d-1. Rectilinear scanning. The first medical radioisotope scanner was devised and constructed for thyroid scanning by Benedict Cassen in 1950 at UCLA (67). The principle of the scanner was that a NaI (Tl) scintillation detector 1" in diameter with a $\frac{1}{4}$" straight bore lead collimator was moving at a constant speed, motor driven, over the neck of a patient. The radiation from ^{131}I in the thyroid was continuously detected. Coupled to the detector was a mechanical printer moving over a sheet of paper. It would print on the paper a dot for each event recorded by the detector. Thus, the density of dots per unit area on the paper was proportional to the ^{131}I present in the corresponding area in the neck. A map of the relative distribution of ^{131}I in the neck was obtained.

In 1952, the straight bore collimator was replaced by a focusing collimator, increasing the resolving power of the detector system (68). To eliminate interference from scattered radiation, Allen suggested the introduction of a pulse height spectrometer to the electronic circuit (69). A major improvement of the obtained image was achieved by the introduction of contrast amplification and photographic recording (70,71). The advantage was, that in addition to the density of dots per unit area on the photographic film, the photographic density of each dot recorded was proportional too to the radiation intensity over that particular area. Another mode, the color scan display, was introduced by Mallard in 1959 (72). The

various intensity levels were printed in different colors. So for a
pre-set count rate of 100%, the colors of the printing ribbon will change
in 12.5% increments. (For example: 0-12.5% white, 12.5-25% black, 25-
37.5% purple, etc.).

The above described factors are the main ingredients of the modern
rectilinear scanner. Since the description of Cassen's model in 1951,
many improvements have been introduced in scanning techniques. While the
original scanner was designed for thyroid scanning with ^{131}I, today more
than 15 organs can be visualized by scanning utilizing a pharmacy of over
50 radiopharmaceuticals. These techniques and drugs have recently been
discussed in two major international symposia in Greece and Oak Ridge
(73,74).

I-d-2. Whole body counting. The first whole body counting was per-
formed with an ionization chamber by Schlundt and co-workers in 1929, to
determine the radium and mesothorium levels in man (75). Due to the low
sensitivity of such a system, whole body counting was not widely used till
the early 50's, when Reines and co-workers described the liquid scintilla-
tion whole body counter (76). In 1955, Marinelli introduced the NaI (Tl)
crystal whole body counting method (77). The advantage of this method
over the liquid scintillation method is about 3 times as sensitive as the
solid crystal. The most commonly used geometrical counting configuration
is the "tilted chair method"--described first by Miller (78). The cali-
bration problems associated with the operation of a whole body counter

have been described and discussed at the Vienna Whole Body Counting Symposium, 1962 (79,80,81). The major aspects are: matching of the phototubes, background index, resolution, stability, efficiency and cross-over.

CHAPTER II. MATERIAL AND METHODS

II-a. The Radiopharmaceuticals.

^{75}Se-selenomethionine supplied for this study was a donation by

E. R. Squibb and Sons Co. and Abbott Laboratories. Colloidal Gold--

^{198}Au was purchased from E. R. Squibb. The radioactive sources used for

the calibration of the whole body counter were absolute standards from

Oak Ridge National Laboratories. Technitium ^{99m}Tc pertechnetate was

"milked" from a Molybdenium ^{99}Mo generator (Squibb).

II-b. The whole body counting facility.

As some of the subjects for this study were to be counted by a low

level counting technique, the first step was the installation and calibra-

tion of a whole body counter.

II-b-1. Installation. The room was constructed of 7.25 inch armor

plate, obtained from the big gun turret top of the battleship U.S.S.

Indiana, constructed prior to the atomic era. The six plates employed had

a combined weight of 65 tons. The top and bottom plates measured eight by

ten feet, the side plates seven by ten feet and the end plates seven by

seven feet. Care was taken to prevent handling of the plates by magnetic

grapples at any time to prevent induced magnetic fields.

The room was pre-assembled and moved to its permanent site as a

unit. The room was placed upon a 12'X14'X3.5' reinforced concrete block

flush with ground level. All materials used within the room were assayed

for radioactivity. Significant activity above background was cause for rejection.

The interior surfaces were covered by 1/8" lead sheet. A standard tilting chair was used for positioning of the patient.

The detector was mounted upon an extension arm with rotational coupling allowing wide angle orientation of the cylindrical axis of the crystal. The extension arm moves laterally on a box girder, the box girder longitudinally on a rail permitting three dimensional positioning of the crystal. Calibration in the X, Y and Z axis is measured by built-in metal measuring tapes. The extension arm is motor operated.

The patient may be observed on two external TV monitors via a TV camera with wide angle lens within the room. Communication with the patient is carried on by two-way intercom. A small TV set with outside antenna coupling is mounted on the crane for patient entertainment (fig. 11).

Fresh air was supplied at a rate of 23.9 cubic feet per minute through the shielded room when operating with closed doors.

The 4" X 8" NaI (Tl) crystal contains 3300 ml of detecting volume. It is enclosed in an unshielded stainless steel container. The crystal is equipped with three matched RCA photomultiplier tubes having calcite faces to reduce ^{40}K background level. This output is fed into a preamp circuit and then into a 512 channel pulse height analyzer equipped with IBM input-output typewriter, Mosely X-Y Recorder and tally tape output and input (fig. 12). The analyzer has a channel summation and processing section.
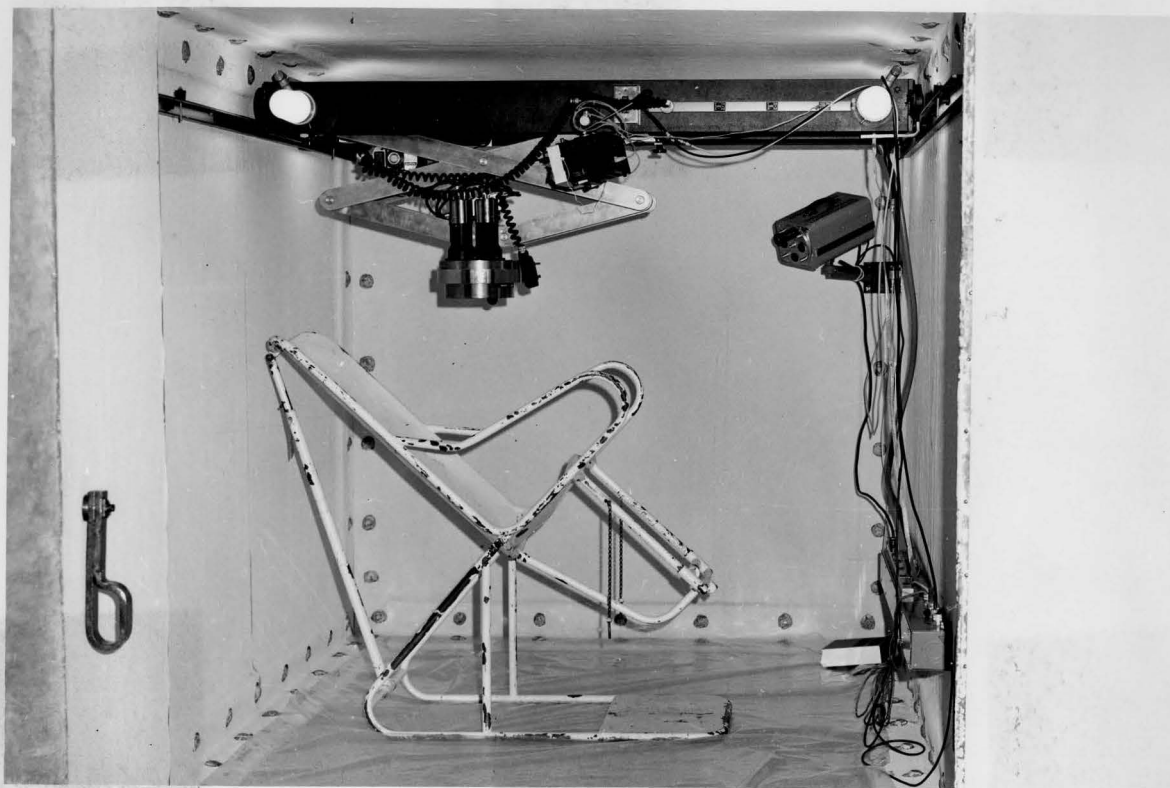
Figure 11. View of interior of the shielded room through the open doors

Figure 12. Multichannel analyzer and readout equipment

II-b-2. Calibration. Successive one hundred minute background counts of the room were taken. The background showed significant fluctuation within relatively short intervals of time (fig. 13). Analysis of the background spectra indicated that the change in background was due to changes in the ^{222}Rn peaks. To establish whether the ^{222}Rn source was internal or external, the room was sealed and the background between .100 Mev and 2 Mev built up to 60% over its initial value. The increase was established to be due to increase in the ^{222}Rn peaks (fig. 13). This result indicated that in spite of all the precautions taken, the ^{222}Rn source was inside the room.

It seemed impractical to try to locate the ^{222}Rn source, so, in order to maintain constant atmospheric conditions in the room, the ventilation system was employed. This addition reduced the fluctuations of the background to within statistics for 100-minute counts over a period of 72^h, around a mean background index of 0.2947 cpm/cc (fig. 14). To check the variation of the background, as due to material contamination or magnetic flux, the detector was moved to the four quadrants of the room and successive 100-minute counts were taken in each location. No significant differences were found (Table I). The magnetic flux within the room was measured and found to vary between 2% to 10% of the normal magnetic flux of the earth field.

To determine the distribution of isoresponse surfaces of the crystal, a 4' X 7.5' pegboard with holes at 2" intervals was placed on the floor. Lucite rods from $\frac{1}{4}$ foot to $5\frac{1}{4}$ feet in length were cut. Their bases fit into the holes of the pegboard, and a ^{137}Cs point source was mounted on the upper
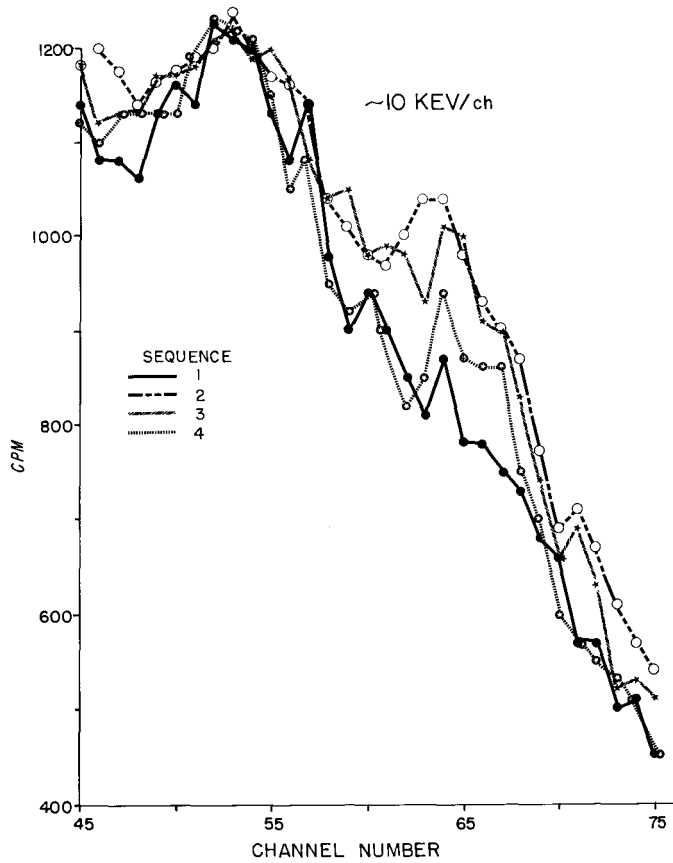
Figure 13. Background variability related to ^{222}Rn level

Variation of background index (B) with position of detector in counting room. (Average of 8 one hundred minute counts)

Position	B (cpm/cc)
Center	.3030
S - E corner	.2878
S - W corner	.2969
N - W corner	.2919
N - E corner	.2989

TABLE I
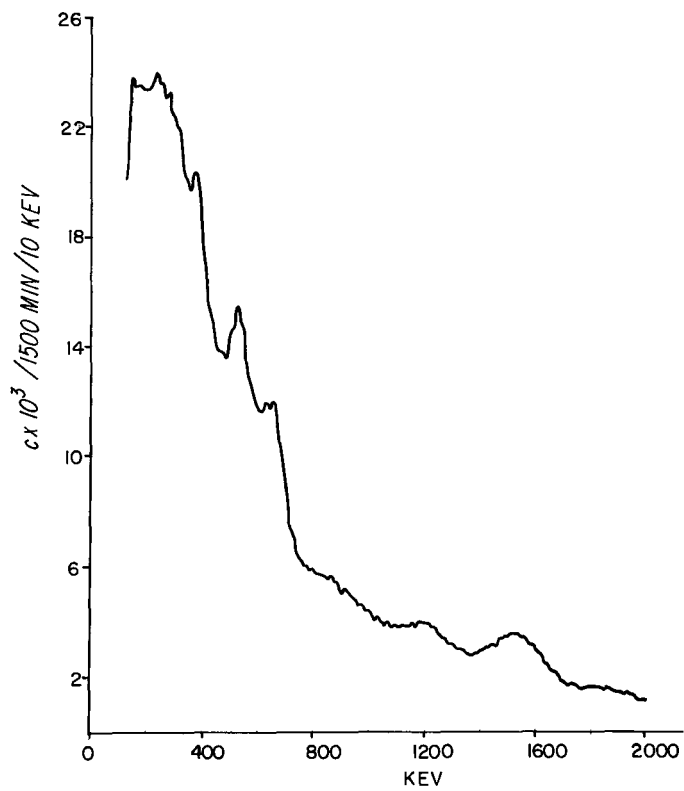
Figure 14. Gamma spectrum of background counts

end of the rods. The various rods were moved throughout the room, and counts were taken at each position. A profile of the isoresponse surfaces is shown in fig. 15. The symmetry and shape appear satisfactory.

Further calibration was accomplished with a Nuclear Enterprise 70 kg phantom filled with 70 liters distilled water. The average background index with this phantom was 0.246 cpm/cc (fig. 16). The sensitivity, background, resolution and isotope interference for ^{131}I, ^{37}Cs and ^{40}K were measured by uniform distribution of the various isotopes in the phantom. All measurements were performed at a 10 kev/channel calibration. The results are summarized in Table II.

"Point" sources (0.1 cc) of ^{131}I, ^{37}Cs and ^{60}Co were introduced into the center of the various parts of the phantom and the point source geometry factors for these isotopes established (Table III). The crystal was positioned at a 50 cm distance from the designated center of the phantom. Using the single chair technique, the geometry factors vary significantly at the extremities and the head, and this variation is less when counting higher energy gamma emissions.

To characterize whole body counters, a figure of merit must be derived. To derive this figure the measurable factors are the sensitivity and the background count for specific isotopes. The efficiency figure for any isotope may be derived by squaring the sensitivity and dividing by the background count. The overall efficiency of the system may be defined as the geometric average of the isotopes used. The three isotopes observed cover the spectral range of interest in whole body counting. The figure
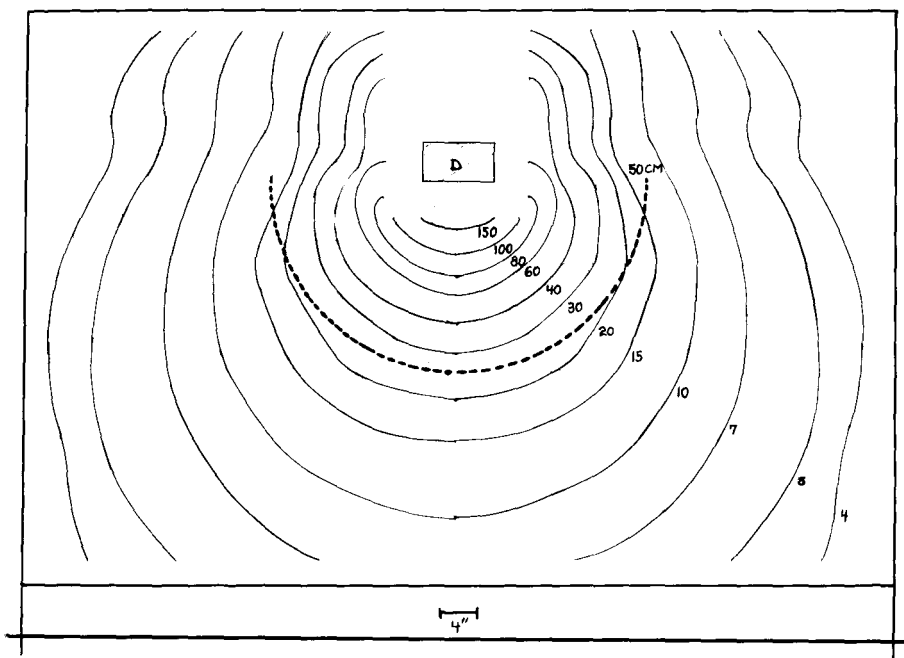
Figure 15. Isoresponse cross-section plot of NaI (Tl) crystal
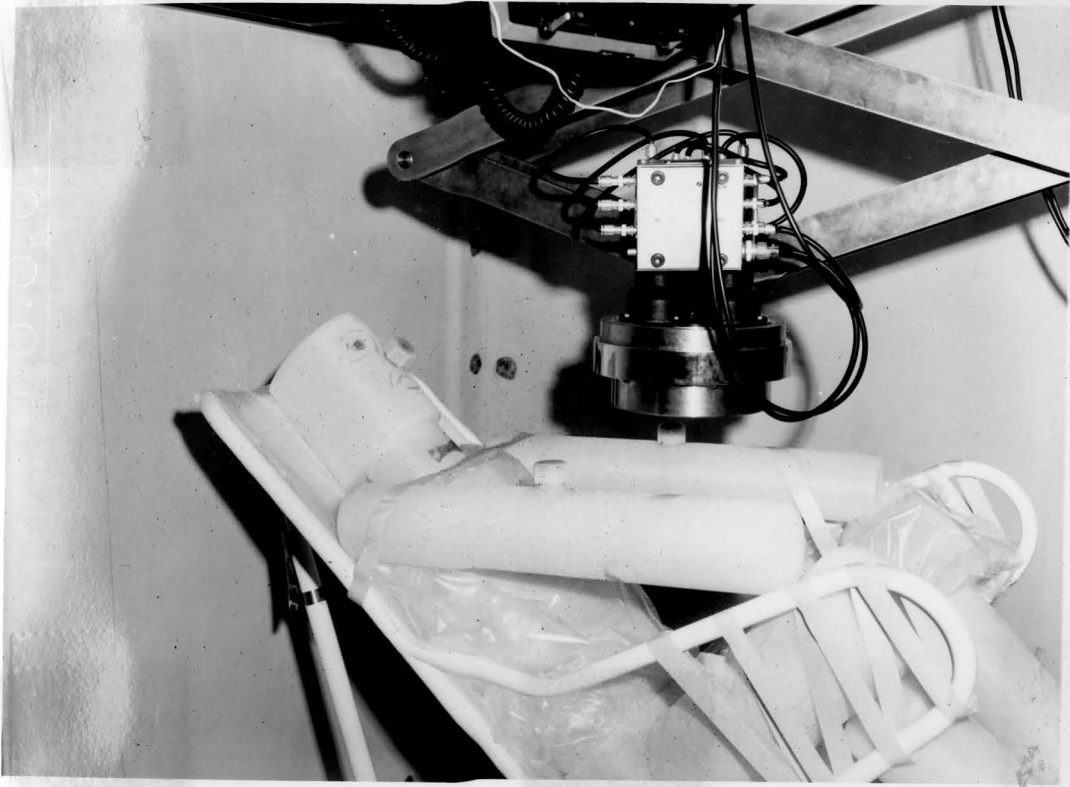
Figure 16. Phantom man in counting position

CALIBRATION DATA FOR THE HINES WHOLE BODY COUNTER

Setting \ Isotope		^{131}I	^{137}Cs	^{40}K
^{131}I η_1^*	1) Sens (s) Res Bgnd (b) Band Eff.	10,018 cpm/μC 13.7% 148 cpm 130 kev 0.67 x 10^6	2097 cpm/μC (contribution of ^{137}Cs cpm at ^{131}I setting)	0.63 cpm/gK (contribution of ^{40}K cpm at ^{131}I setting)
^{137}Cs η_2^*	1) Sens (s) Res Bgnd (b) Band Eff.		15,089 cpm/μC 8.9% 158 cpm $\approx$ 260 kev 1.44 x 10^6	
η_3^*	1) Sens (s) Res Bgnd (b) Band Eff.			0.63 cpm/gK 8.9% 61 cpm 170 kev 6.5 x 10^{-3}
B.I. Background Index		0.2960 cpm/cc		
$\eta = \sqrt[3]{\eta_1^* \times \eta_2^* \times \eta_3^*}$ Overall Eff.		1840		
Fig. of Merit $M = \dfrac{\eta}{B.I.}$		6216		

$\eta_i^* = \dfrac{si^2}{bi}$

1) Isotope uniformly distributed throughout 70 kg phantom.

TABLE II

Geometric factors for ^{131}I, ^{37}Cs, ^{60}Co point sources at various locations in phantom.

Isotope Location	^{131}I	^{37}Cs	^{60}Co
Head	0.17	0.27	0.31
Neck	0.77	1.04	1.00
Chest	1.00	1.00	1.00
Pelvis	0.64	0.84	0.70
Thigh	1.07	1.39	1.13
Shin	0.32	0.64	0.48
Arm	1.42	2.20	1.90

TABLE III

of merit (M) is then defined as the overall efficiency divided by the integral background over this spectral range.

(M) is specifically defined as follows:

$$M = \frac{\eta}{B}$$

where η_i is the overall isotope efficiency:

$$\eta_i = (\eta_{i_1}^* \times \eta_{i_2}^* \times \eta_{i_3}^*)^{\frac{1}{3}}$$

η_i^* is the efficiency of individual isotopes in their respective energy bands

$$\eta_i^* = \frac{s_i^2}{b_i}$$

s_i is sensitivity of cpm per μCi [1]

b_i is background

where B is the background index the integral background in counts per minute per cc of crystal. The integral band measured was 0.1 to 2 Mev.

II-c. Development of the multi-energy isotope scanner.

One of the objects of this study was to observe in vivo distribution of ^{75}Se-selenomethionine in man by means of rectilinear scanning. As mentioned in the introduction, one of the limiting factors for this procedure was the relatively high concentration of ^{75}Se-selenomethionine in the liver, making it extremely difficult to observe other organs in the

---

[1] In case of ^{40}K, cpm per g. potassium

abdominal and thoracic region. Therefore, a commercially available scanner (Picker Magnascanner V) was converted to be able to subtract radiation of different energies from different organs and display them in different colors. Ultimately a tape recording cathode ray display system was adapted for improved color image presentation.

II-c-1. The block diagram. The block diagram of the system is illustrated in fig. 17. The following parts are added to the conventional scanner: input mixing box, a dual channel analyzer, an output mixing box, two dual ratemeters, a DC-frequency converter and a DC-isolator. An additional pulse amplifier was wired into the scanner ratemeter chassis (EXT.PLS.-AMP on fig. 17), to permit independent recording on the photo and print systems. The modes of operation of the modified scanner are selected by turning a single 6-deck rotary switch, which is also shown in fig. 17. Fig. 18 is a photograph of the modified scanner. An additional modification is the introduction of a "one-way circuit" to the mechanism of the scanner. This circuit permits the scanner to record while moving in one direction only, returning over the same line at 200 cm/min speed. Since scalloping results from a delay in print-out of alternate scan lines due to the factor of time constant, this type of scanning eliminates scalloping completely, thus making high-speed, slow time constant scanning possible. The relatively slow time constant (1 sec) is necessary for subtract scanning to permit sufficient time for the subtraction event.

Figure 17. Block diagram of the modified scanner and switching arrangement for various modes of operation
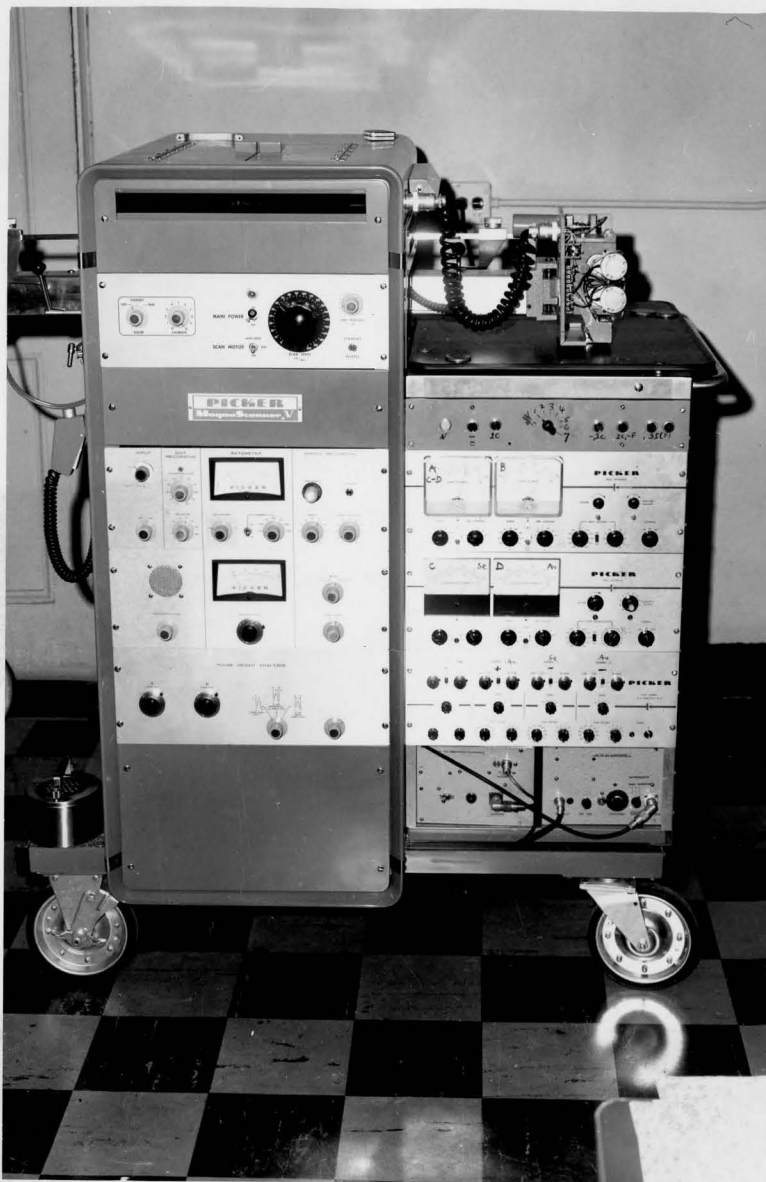
Figure 18. Photograph of the modified scanner. Modifications on right

II-c-2. Logic and procedure.

Position 1. In this position the scanner will function as a conventional color scanner, only the original components of the scanner being included in the circuit.

Position 2. Pulses of different energies from two isotopes are discriminated by two pulse height analyzers, fed to individual components of a dual ratemeter, subtracted one from the second, and fed through a DC to a frequency converter (fig. 19), to the $-\frac{1}{4}$ V input of the scanner ratemeter. The difference of the pulses may be recorded on both the photo and mechanical recording devices. The major application of this mode of scanning appears to us to be for pancreatic scanning. ^{75}Se-selenomethionine and colloidal ^{198}Au are administered to the patient simultaneously. One channel detects the 411-keV ^{198}Au gamma emission the other detects the 270 and 280 keV ^{75}Se-selenomethionine gamma emission, each through a 100 keV window. Phantom studies proved that this system is quite effective.

Figure 20 shows top (a) and later, (b) scanning of a phantom without subtracting, and (c) and (d) are respective scans, subtracting the ^{198}Au signals from the ^{75}Se-selenomethionine signals. Our phantom system consists of a Marinelli Beaker filled with 90 μCi ^{75}Se-selenomethionine and 90 μCi ^{198}Au in 900-cm^3 fluid, and a 150-cm^3 plastic bottle which contained 75 μCi ^{75}Se-selenomethionine. This bottle inserted into the hollow part of the beaker. Figure 20 shows clearly that the signals from the surrounding beaker may be completely eliminated electronically.

The detector is directed over the maximum ^{198}Au count of the liver.
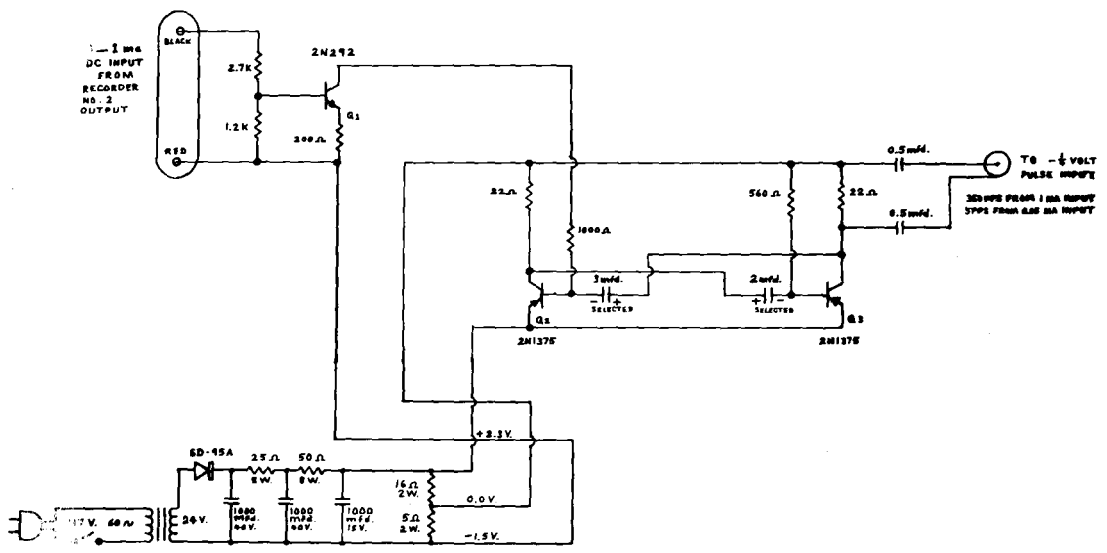
Figure 19. Schematic diagram of the DC-frequency converter
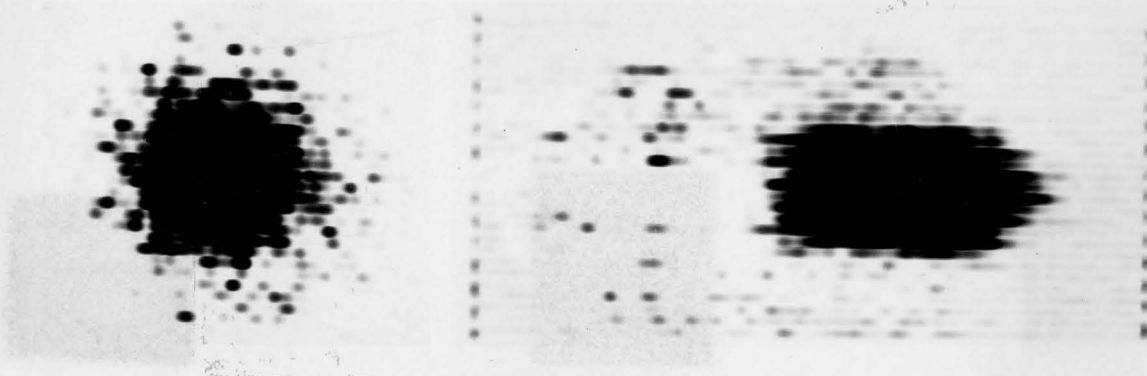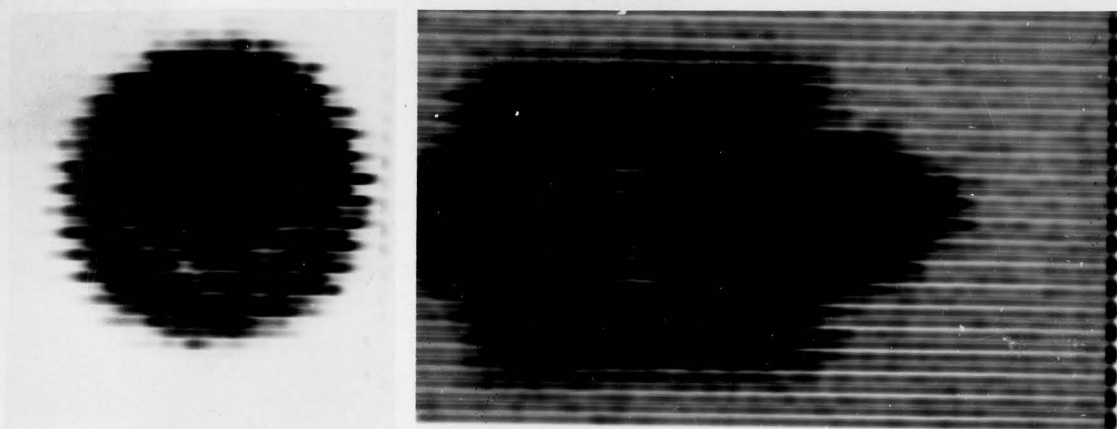
Figure 20. (a) End on scan of ^{75}Se activity in two concentric containers, visualizing ^{75}Se gamma photo peak. (b) Scan of ^{75}Se activity in two concentric containers, visualizing ^{75}Se gamma photo peak. Lateral view. (c) End on scan of ^{75}Se activity in two concentric containers, outer container neutralized by subtraction of ^{198}Au activity from ^{75}Se activity. (d) Scan of ^{75}Se activity in two concentric containers, outer container neutralized by subtraction of ^{198}Au activity from ^{75}Se activity. Lateral view.

The patient then receives 250 μCi of ^{75}Se-selenomethionine intravenously.
The count rate for ^{198}Au and ^{75}Se-selenomethionine are observed simul-
taneously on the individual count-rate meters. Within 10 to 15 min.,
the ^{75}Se-selenomethionine count stabilizes. The amplitude of deflection
of the two isotopes are equated, adjusting the respective channel widths,
and the ^{198}Au count placed in negative mode. Scanning at a speed of 60 cm/
min and at 4-mm line intervals, the scan can be completed in 20 min.

Figure 21 (a) shows a pancreas scan carried out by the regular method,
without subtract, and (b) shows the same patient scanned by the subtract
method.

Position 3. In this position, two isotopes emitting photons of
different energy levels may be scanned simultaneously and a color display of
the distribution of each of the isotopes in a different color obtained. The
overlying parts will appear on the scan in intermediate shades of the two
colors. Pulses from the preamplifier are fed into a dual channel analyzer.
The outputs of the two channels are split, feeding into a dual ratemeter
and a mixing circuit consisting of two diodes to prevent feedback from one
channel to the other. The pulses from the mixing circuit are fed through
the scanner ratemeter and drive the stylus. The ratemeter outputs are
subtracted one from the other by a built-in circuit. The difference, which
may be positive or negative, used to subtract one isotope from the other may
now display the subtracted isotope in one color and the positive in another
color by driving the scanner's color control through a DC isolator designed
and constructed in this laboratory. This isolator is essential, as the DC
output of the subtractor and the DC input of the color drive are isolated.

a
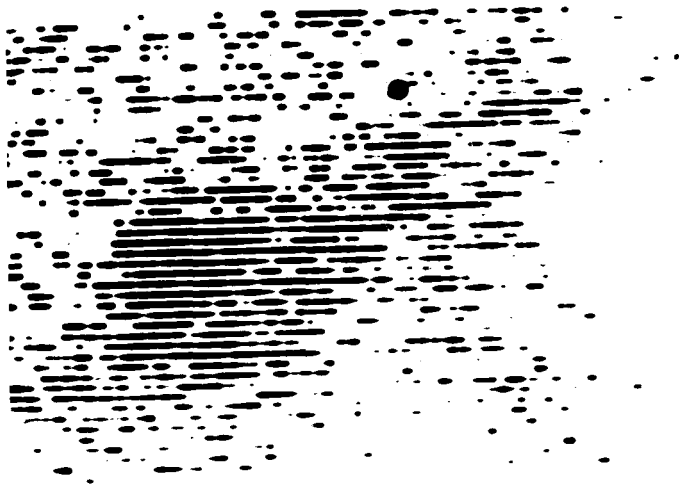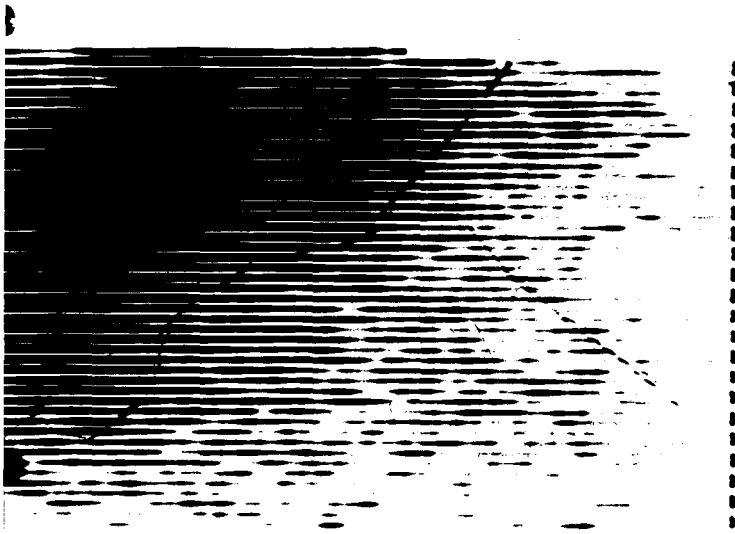
b

Figure 21. (a) Pancreas scan using ^{75}Se-selenomethionine alone.
(b) Same patient scanned by the subtract method.

DC INPUT
FROM
SUBTRACT
CIRCUIT

47 K
27 K
15 K

COLOR
RANGE
SELECTOR

330 K

330 K

100 K   91 K

160 K

1.5 V.

AMPEREX
6977

15

OPTICAL
COUPLING

1.5 V.   30 V.

COLOR
CENTERING ADJUST

CDS-10

43 K   470 K

250 K

36 K

39 K

DC
OUTPUT
TO COLOR
DRIVE

67.5 V.

SCALE:
DATE: 5-19-65

APPROVED BY
m. Ben-Porath

DRAWN BY
REVISED

DC TO DC CONVERTER

DRAWING NUMBER
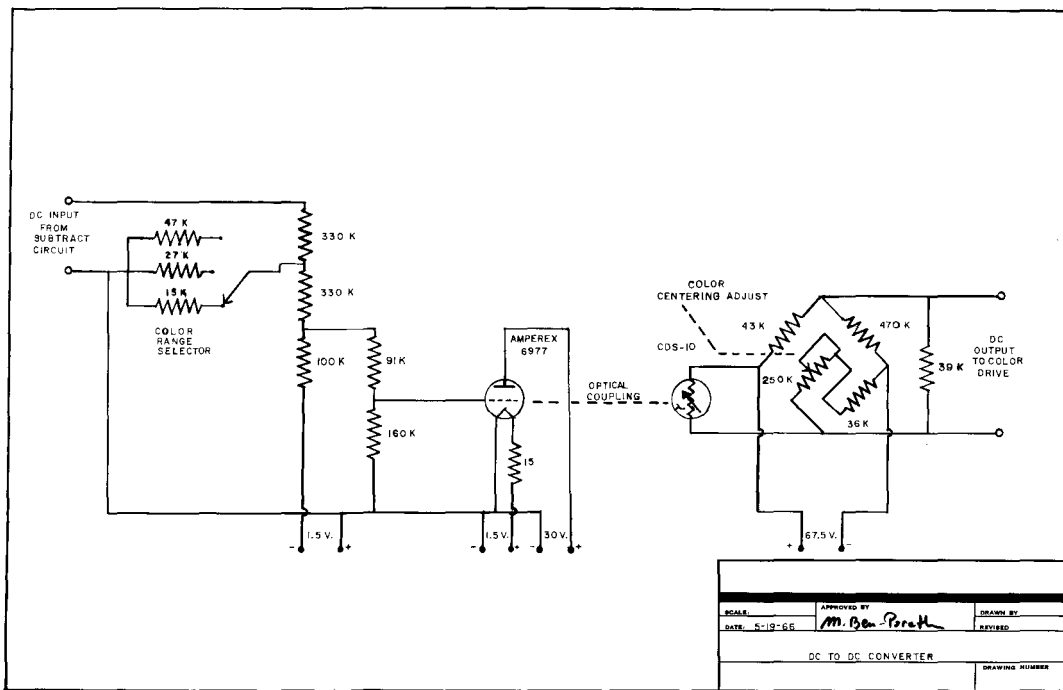
Figure 22. Schematic diagram of the "color calibrate" circuitry

The DC isolator schematic diagram is shown in fig. 22. In operation, the DC output of the subtract circuit is connected to a #6977 Amprex light source. Any change in the DC output, positive or negative, will alter the light intensity of this lamp. The light output is measured by a cadmium sulfate (cds) cell; the DC output of the cds cell drives the color control. This output is proportional to the light output and thus proportional to the relative output from the two ratemeters.

The standard color tape of the scanner consists of seven usable colors, with black at one extreme and dark red at the other; purple, blue, green, orange and a light red are intermediate colors. The color tape has been modified using only two colors—blue and red, and four shades of each, diminishing in darkness from the extremes to the center. The range of color is controlled by the scanner "color calibrate" potentiometer control and by the resistor switch in fig. 22. The center color is set by the potentio-meter in fig. 22. If only pulses of energy A are detected, the color band will be deflected to one extreme and the pulses will be recorded in color A. If only pulses of energy B are detected, the color ribbon will be deflected in the opposite direction and only color B will be printed. If pulses of both energies are detected, the color ribbon will move between the extremes printing out intermediate shades of the two colors. If A is greater than B, the lighter shades of color A will be printed, the darker shades indicating the magnitude of the difference. If A is less than B, shades of color B will be printed. The intensity of the counts is indi-cated by the density of impulses printed, which is controlled by the sum of A B.
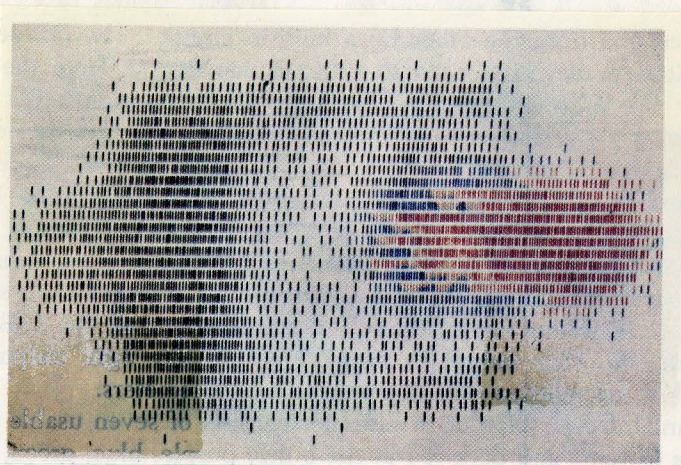
Figure 23. Color scan energy modulation of the phantom in Fig. 20.
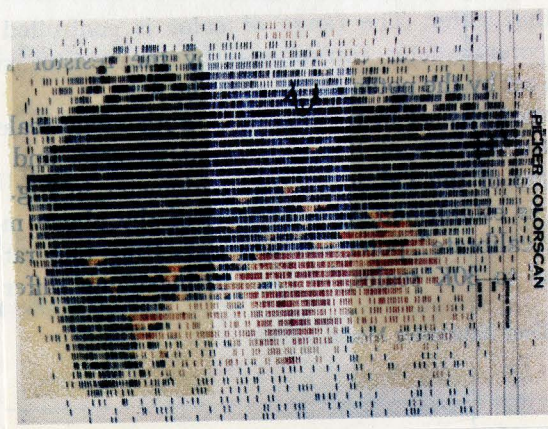
Figure 24. Liver and pancreas visualized in separate colors: ^{75}Se + ^{198}Au signals in one channel (blue), ^{75}Se signals alone in second channel (red).

Figure 23 shows the energy-color scan of a phantom, consisting of 50 μCi ^{198}Au in a Marinelli Beaker and 50 μCi ^{75}Se-selenomethionine in a cylindrical container inserted 3/4 into the hollow part of the beaker. The gold is printed out in black, the selenium in red, and the overlapping part in the intermediate colors. Figure 24 is a scan of the liver containing ^{75}Se-selenomethionine and ^{198}Au shown in blue and the pancreas containing ^{75}Se-selenomethionine in red.

Position 4. In this position, both the subtract and the two color circuits are activated. The net output of the subtract is fed from the DC-frequency converter to one of the two ratemeters of the color control dual ratemeter and to the input of the output mixer box. In this setting scanning two isotopes, one will be displayed in one color and the "subtract" of the two in a second color. This factor is particularly useful if, for instance, the pancreas and the liver are to be displayed. Then the ^{198}Au will be displayed in one color and the extrahepatic ^{75}Se-selenomethionine minus ^{198}Au pulses in the second color (fig. 25).

By means of this method it was possible for the first time to demonstrate that hepatomas may be visualized by scanning as positive lesions (fig. 26).

Position 5. It is possible to simultaneously visualize two organs in separate color on paper and a subtract scan demonstrating a single organ, with the other subtracted, on film.

Position 6. In this mode of operation, two isotopes drive the color control and stylus as described in position 3, while the pulses of a third are fed through the scanner pulse height analyzer, bypassing the stylus
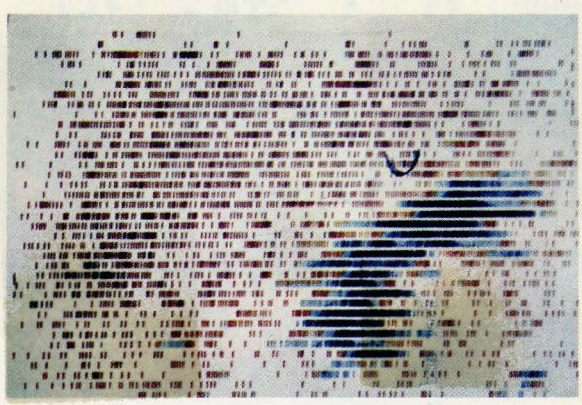
Figure 25. Liver and pancreas: ^{198}Au signals from liver in red, ^{75}Se-^{198}Au signals from pancreas in blue.

Figure 26. The first hepatoma ever to be visualized as a positive scan (in blue) by the dual color subtract method.

mechanism through the external pulse amplifier and recorded on the film.

Other technical modifications eliminated scalloping by printing while scanning in one direction only, the detector returning at high speed without printing. Further modification has resulted in significant simplification of the circuitry seen in the block diagram (fig. 27). Despite the prolongation of scanning time using this method, the quality of the scan is improved. The standard color scanner is altered by addition of a single channel pulse height analyzer and a two-contact relay. In operation the probe, when moving from left to right, trips the carriage limit (probe reverse) micro switch at the end of a scan line. In addition to reversing scan direction, a relay is activated permitting only pulses from PHA 1, set for isotope A, to be recorded in color A in the following line. At the end of that line, the second carriage limit micro switch activates PHA 2 set for isotope B to be recorded in color B in the subsequent line. The two sequences alternate throughout the scan. Thus, one isotope will be recorded in a specific color while the probe is scanning in one direction and the second isotope in a different color, while the probe is scanning in the opposite direction. To prevent loss of space density, one-half of normal spacing should be employed, so that each isotope will be scanned at normal spacing (e.g. if the normal spacing for liver and pancreas scanning is 4 mm, a spacing of 2 mm is used with this method). Scalloping is also eliminated using this technique, as each isotope is scanned in one direction. Displacement of the images in each color occurs relative to each other. Being a function of scanning speed and time constant,

PULSE HEIGHT ANALYZER No I

MODE SWITCH [1] [2]

I TWO ISOTOPE SCAN

[2] SUBTRACT-AND-ONE ISOTOPE SCAN

DUAL RATEMETER IN SUBTRACT MODE

MIXER

DC to AC CONVERTER

SERVO POTENTIOMETER COLOR CALIBRATOR

RED

BLUE

± V INPUT

SCANNER RATE-METER → STYLUS

PULSE HEIGHT ANALYZER No·2

PROBE

TO SCANNING ARM CARRIAGE LIMIT SWITCH.

K_3

RELAY COIL K_3 IS ENERGIZED IN ONE DIRECTION ONLY, AS CONTROLLED BY THE CARRIAGE LIMIT SWITCH·

<u>Figure 27.</u> Circuit diagram of "one way-one isotope" scanner modification.
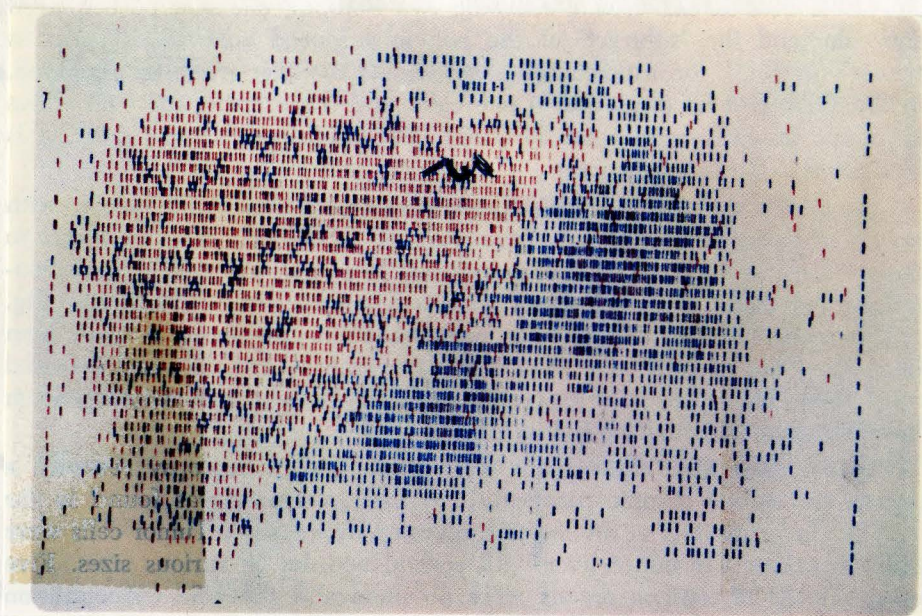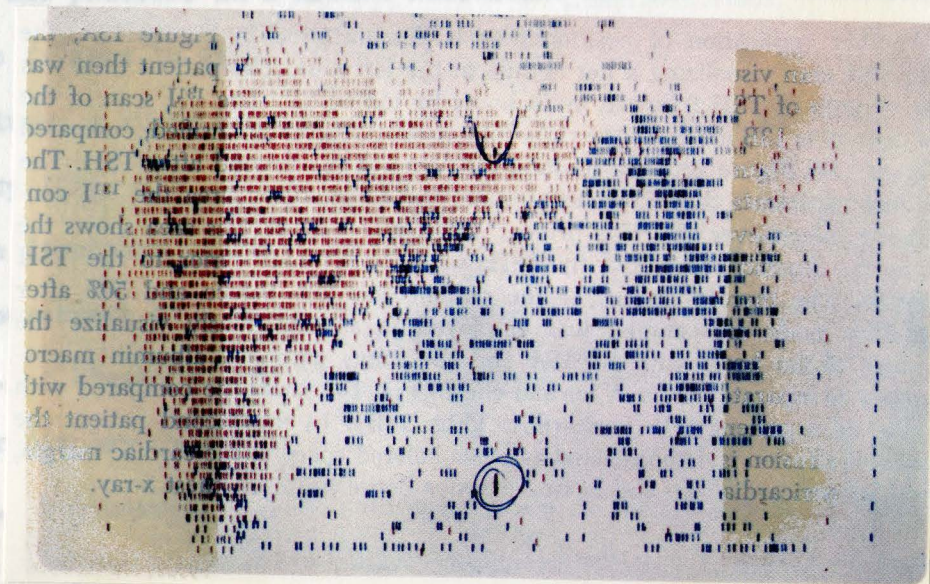
Figure 28. (a) Normal liver and pancreas visualized by scanning modification in Fig. 27. (b) Normal liver and carcinoma of the pancreas visualized by scanning modification in Fig. 27.

it can be calculated:

$$D = T \times S$$

where D = displacement in cm

T = time constant in seconds

S = scanning speed in cm/second

(e.g. If T = 0.1 second, S = 1 cm/second, D = 0.1 X 1 = 0.1 cm in each direction, which is negligible).

The subtract circuit described in position 2 may also be used with this method, allowing the "subtract scan" to be visualized in one color and one of the two isotopes in a second color. A representative scan of a liver and pancreas in a normal individual and one with carcinoma of the pancreas is seen in fig. 28 a and b. To accomplish the subtract mode, a mode switch, a DC to AC converter and a dual ratemeter are added to the circuitry (fig. 27).

The displayed color image was further improved by the introduction of a four-track tape recorder coupled to a CRT display unit into the circuit. A block diagram of the essential connection of the scanner-recorder-display system is shown in fig. 29. A photograph of the system in fig. 30. A conventional scanner was used, to which one additional single channel analyzer was added. The outputs of analyzer one and two are recorded on channel 3 and 4 respectively. If a subtraction scan is desired, switch S_1 is flipped into position 2. In this position the information from analyzer one will be recorded on channel 3 and the "subtract output" (information from analyzer two less the information from analyzer one) on channel 4. The x and
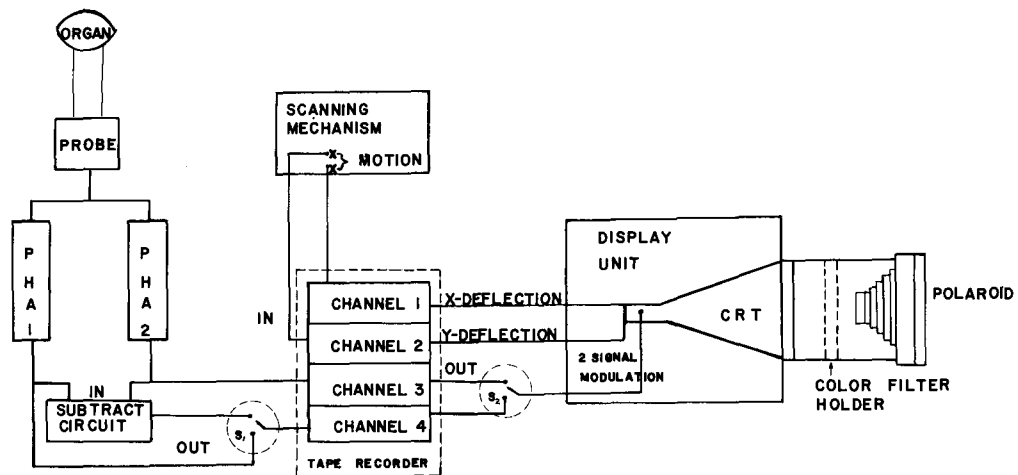
Figure 29. Block diagram of the scanner-tape recorder-display unit system.

Figure 30. Photograph of the tape recorder-display unit

y movements of the scanner are recorded on channels 1 and 2 respectively.
The recorded information is played into the readout unit and will be dis-
played on a white phosphor cathode ray tube (CRT). The x and y deflection
of the CRT beam are controlled by channels 1 and 2 of the tape. The beam
intensity (z axis modulation) is proportional to the signal output from
channels 3 or 4, depending on the position of S_2. The CRT display is
continuously monitored by a Polaroid camera loaded with a color film.
A filter holder was built between the CRT screen and the camera, where
filters of various colors may be mounted. When the information from
channel 3 is played back filter A is used to obtain a picture of the
distribution in color A. Then channel 4 is played back, recorded on the
same film, using filter B. The distribution of isotope B will thus be
displayed in color B. The overlay areas will appear in a mixture of colors
A and B, distinct from A or B. The replay is carried out at a speed 16
times faster than the recording (60" per minute vs. 3.75" per minute).
The tape used is a standard type 3M-203 tape. The replay procedure may be
repeated as many times as desired changing the intensity, contrast and
background cut-off settings for each channel. This permits the achieve-
ment of optimal displays as well as detailed analysis of the organs scanned.

II-d. The subjects studied.

II-d-1. Total body biological half life. The biological half life
of ^{75}Se-selenomethionine was determined by whole body counting in 3 groups
of subjects, all males.

A- Controls: Nine clinically healthy volunteers from the personnel

DIAGNOSES AND PHYSICAL CHARACTERISTICS OF THE SUBJECTS FOR

TOTAL BODY HALF LIFE EVALUATION

SUBJECT	DIAGNOSIS	AGE	WEIGHT (kg)	HEIGHT (cm)	RACE
B.K.	Normal	46	82	178	C
E.G.	Normal	49	111	178	N
T.K.	Normal	45	80	173	C
E.K.	Normal	44	73	173	C
J.G.	Normal	40	95	168	C
J.S.	Normal	41	86	180	C
E.B.	Normal	44	84	178	N
J.K.	Normal	41	77	180	C
M.B.	Normal	47	63	185	C
E.S.	Lymphosarcoma	72	69	180	C
M.T.	Hodgkin's dis.	57	65	180	N
M.K.	Ret. cell sa.	48	68	175	C
H.R.	Lymphosarcoma	57	73	163	C
M.Z.	Hodgkin's dis.	27	77	175	C
E.F.	Chr. pancrtis.	60	93	183	C
W.E.	Chr. pancrtis.	40	70	175	C
A.R.	Chr. pancrtis.	45	65	180	N
J.D.	Pancr. insuff. & severe diab. mellitus	47	57	178	C

TABLE IV

of the Research Service of the V.A. Hines Hospital.

B- <u>Malignant Lymphomas</u>: Five patients with various types of malignant lymphomas from the Hematology ward, V.A. Hines Hospital.

C- <u>Pancreatic Diseases</u>: Four patients with non-neoplastic pancreatic diseases from the Gastrointestinal ward, V.A. Hines Hospital.

Table IV summarizes the physical characteristics and diagnoses of the subjects.

The malignant lymphoma patients did not receive chemotherapy with antimetabolites throughout the duration of the study.

<u>II-d-2</u>. In Vivo and necropsy studies. Two hundred and twenty patients were scanned for this study. All patients were males ranging 30-76 years. Seventy were found to be clinically normal subjects. The others suffered from various diseases as listed in Table V. One hundred and nine of the 220 were evaluated by the dual isotope scanning method with mechanical color display, the other 111 by the tape recorder display.

Three patients were counted for the evaluation of the biological half life of ^{75}Se-selenomethionine over various areas of the body. The areas are shown in fig. 31.

One patient died of hepatoma 52 days following the administration of 250 μci ^{75}Se-selenomethionine. Tissue samples were obtained from the pancreas, kidneys, normal liver tissue and the hepatoma. The tissues were weighed and assayed for radioactivity with a scintillation well counter. Another patient died of bronchogenic carcinoma 72 hours following

DISTRIBUTION OF PATIENTS BY DIAGNOSIS AND ORGANS SCANNED

	PANCREAS	LIVER	MYOCARDIUM	BRAIN
Clinical normal	70	70	10	2
Ca of pancreas	20	20	--	--
Pancr. insuff.	39	39	4	1
Cirrhosis	34	34	1	--
Pancreatitis	16	16	1	--
Other GI disorders	36	36	2	--
Brain lesions	--	--	--	3
Hepatoma	5	5	--	--
TOTAL	220	220	18	6

TABLE V

the administration of a similar dose. Tissues from most of this patient's organs were assayed for radioactivity. The tissues are listed in Table VI.

II-e. Procedures.

II-e-1. Half life studies. Following a shower, a special gown was assigned to each subject. The gown was previously tested for radioactive contamination. This was necessary to assure that radioactivity detected while counting the patient was not from extrinsic sources. Next the subjects were counted by the whole body counter to determine their natural radioactivity and to check whether they contained any traces of radioisotopes that might have been previously administered to them for other procedures. These counts were considered as base line readings. Two μci ^{75}Se-selenomethionine were administered intravenously to the subjects. Ten minutes later they were counted. Each subject was counted three times, 5 minutes each, and the sum of the three counts divided by 15. This reading was considered as the zero time 100% reading for each individual. A standard test source of ^{75}Se-selenomethionine was counted preceding and following the patient in order to check the stability of the counting system. This standard reading also served for correction of the readings from the subjects for radioactive decay. The subjects were counted one hour, 4 hours, one day and then every second or third day for 3 weeks, then once a week for the next 6 weeks, then monthly and after 100 to 120 days, every 100 days approximately, up to one year.

Tissue concentrations and dosimetry 72 hours following 250 μci ^{75}Se-selenomethionine.

ORGAN	WT.(gm)	% DOSE 100 gm	TOTAL %	C ($\frac{\mu C}{gm}$)	C × T_e	g	(rads) D
Kidney	350	1.80	6.3	.045	1.08	41	3.85
Liver	1750	1.62	28.4	.041	0.98	68	5.30
Pancreas	80	1.13	0.9	.028	0.67	25	1.66
Spleen	100	0.90	0.9	.023	0.55	28	1.48
Gallbladder	20*	0.70	≤ 0.1	.018	0.43	20	0.92
Bile	10*	0.70	≤ 0.1	.018	--	--	--
Adrenal glands	15	0.67	≤ 0.1	.017	2.00	15	3.64
Thyroid	20	0.50	≤ 0.1	.013	1.56	20	3.34
Prostate	25	0.40	≤ 0.1	.010	1.20	23	2.28
Intestines & Stomach	1750*	0.36	6.4	.010	0.17	68	0.92
Solid Tumor	550	0.38	2.1	.010	1.10	47	4.38
Lung	3300	0.34	11.2	.0085	1.00	105	7.96
Metastatic Lymph Node	30	0.33	≤ 0.1	.0083	1.00	24	2.41
Testes	40	0.25	≤ 0.1	.0063	0.75	24	1.81
Pericardium	80*	0.25	0.2	.0063	0.75	25	1.87
Myocardium	420	0.24	1.0	.0060	0.72	44	2.77
Brain	1360	0.22	3.0	.0055	0.66	65	3.64
Blood	5000*	0.22	11.0	.0055	--	--	--
Urinary Bladder	150	0.20	0.3	.0050	0.12	31	0.35
Diaphragm	200*	0.15	0.3	.0038	0.46	34	1.43
Aorta	100*	0.13	≤ 0.1	.0033	0.40	28	1.07
Skin	6100*	0.09	5.5	.0022	0.27	40	0.95
Skeletal Muscle	30,000*	0.06	18.0	.0015	0.20	58	0.95
Bone	7000*	0.04	2.8	.0010	0.12	40	0.42

*Estimated weight

TABLE VI

II-e-2. Scanning procedures.

Method one. The patient is prepared by fasting overnight. Break-
fast consists of 300 grams of gelatin dessert containing 4.5 grams of
protein which is fed because of its relatively low methionine content.
In the presence of abundant other amino acids, selenomethionine concen-
tration in the pancreas may be enhanced. Thirty minutes following this
meal, the patient is administered 100 μci of ^{198}Au colloid by intra-
venous injection. Seventy-five minutes after breakfast, the patient
received 1/6 to 1/4 grains of morphine sulfate, the dose depending upon
the patient's weight and tolerance, to assure constriction of the
sphincter of Oddi (43). Fifteen mg of propanthelin bromide (Probanthine)
were administered at this time to decrease the fluid volume of the
pancreatic secretion (95). The two agents used simultaneously should
prevent phenomena related to increased intraluminal pressure in the
pancreatic ducts (96), without altering selenomethionine accumulation.

Method two. The patient received a regular breakfast followed in
30 minutes by 100 μci of ^{198}Au colloid by intravenous injection.

Common to the two methods, 90 minutes to 120 minutes after breakfast,
the patient is placed supine with the detector over the right lobe of
the liver. Two hundred and fifty microcuries of ^{75}Se-selenomethionine
are administered intravenously. The count rate for ^{198}Au and ^{75}Se-seleno-
methionine are observed simultaneously. Within 10 to 15 minutes the ^{75}Se-
selenomethionine count stabilizes. The amplitude of deflection of the two
ratemeters is equated by a balancing circuit or by window width adjustment.
The ^{198}Au is subtracted. The patient is scanned at a speed of 60 cm per

minute at 4 mm line interval. The scan is completed in 20-40 minutes, depending on field size. The equality of the ^{198}Au counts and the ^{75}Se-selenomethionine counts are rechecked over the right lobe of the liver, adjusted if necessary, and the scan may be repeated.

Method two appears equally effective when compared with method one and was soon used exclusively.

The subtract system was evaluated by several means. The initial evaluation was determined upon a model system. The model pancreas was a plastic container filled with 75 μci of ^{75}Se-selenomethionine solution, while the liver was represented by a Marinelli-type plastic container with a hollow center. This container was filled with a solution of 90 μci of ^{198}Au and 90 μci of ^{75}Se-selenomethionine.

The system was subsequently tested upon 25 male subjects subjected to the regimen and dosage above described. The pancreas was scanned serially after administration of the labeled selenomethionine for periods up to 30 hours. Fourteen patients have been subjected to three or more serial scans. The anatomical configuration has been noted in the scans studied.

One hundred and nine of the 220 scans for pancreatic disorders were carried out by the dual color energy modulation technique described in II-c-2. With this method ^{75}Se-selenomethionine minus ^{198}Au was printed out with the scan traverse in one direction, and ^{198}Au was printed out in the contrasting color as the scan traverse returned in the opposite direction. The scan spacing of 2 mm interdigitated the scan lines. In both channels, 10% of the background was erased. The subtract and two color

circuits were utilized. The scanning technique was described in II-c-2.
Scans extended from the nipple line to the iliac crest. Thirty-six
patients were free of known pancreatic or hepatic disease, 18 had
unconfirmed diagnosis by the criteria described below, 10 had carcinoma
of the pancreas, 19 had chronic pancreatitis with exocrine insufficiency,
and 17 had Laennec's cirrhosis. Finally, eight of the nine patients
listed in Table VII as "Other Diagnoses" were cases of recurrent pancrea-
titis, and the ninth had a massive intraperitoneal hepatoma following
splenectomy. Carcinoma of the pancreas was proven by subsequent laparo-
tomy or necropsy. Chronic pancreatitis was evaluated by a positive secre-
tin-pancreozymin test, x-ray demonstration of pancreatic calcification,
glucose tolerance determination, and steatorrhea as determined by the 72-
hour stool fat. The diagnosis of cirrhosis was based upon clinical findings
and confirmatory liver biopsy. Many of the cirrhotic patients had histories
of alcohol ingestion, but none had laboratory or clinical evidence of
pancreatic disease.

The factors evaluated were anatomical configuration of the liver
and pancreas and also of the spleen when present in the scan. This
included the presence or absence of diffuse or focal defects in the liver
and pancreas. The relative level of ^{75}Se-selenomethionine not cleared by
the liver or pancreas and visualized outside of this organs was also
estimated. The specific criteria for determination of normal pancreas,
carcinoma of the pancreas, chronic pancreatitis and cirrhosis are des-
cribed in Chapter III (Results). The problems of distinguishing between
the various diagnoses are included in Chapter IV (Discussion).

EFFICACY OF DIAGNOSIS OF PANCREATIC DISEASE BY DUAL CHANNEL SCANNING

CONFIRMED DIAGNOSIS	DIAGNOSIS FROM SCAN				
	NO.	NORMAL	CA	INSUFFI-CIENCY	CIRRHOSIS
Clinical Normal	36	31	0	4	1
Carcinoma of Pancreas	10	2	8	0	0
Pancreatic Insufficiency	19	6	0	12	0
Cirrhosis	17	4	3	0	10
Other Diagnosis					
Acute recurrent pancreatitis	8	4	0	4	0
Postoperative splenectomy with massive intraperi-toneal hematoma	1	0	1	0	0
Diagnosis Unconfirmed	18				
TOTAL	109				

TABLE VII

The other 86 pancreas scans were performed by the tape recording method described in II-c-2. The criteria for diagnosis remained unchanged, but its accuracy appeared to be improved, due to the superior quality of the images obtained and the possibility to "rescan" the "patient" from the tape, changing the contrast and intensity settings of each channel, for optimal visualization.

All the myocardium scans were performed on patients referred for pancreatic scans. No special preparation was needed. The scanning was started immediately following the completion of the pancreas scan.

For brain scans, the normal subjects were from the same group of patients. After the pancreatic scan was completed, they received a dose of 5 mci ^{99m}Tc-pertechnetate, and ten minutes later the brain scanning started. The distribution of each isotope was displayed in a different color.

Both, the myocardial and brain scans were carried out by the tape recording technique.

II-e-3. Directional counting. The three patients on whom the biological half life in various areas of the body was determined were counted by the "directional method". A 2" NaI (Tl) crystal with a flat field collimator composed the detector system. The counting system was a RIDL-γ-spectrometry modular system. The patient received 50 μci ^{75}Se-selenomethionine intravenously and counts were registered for 90 seconds over each area. The patients were counted 15 minutes following the injection, one hour, 4 hours and then on days 1,2,3,6,7,8,9,10,13,14,21, and 28.
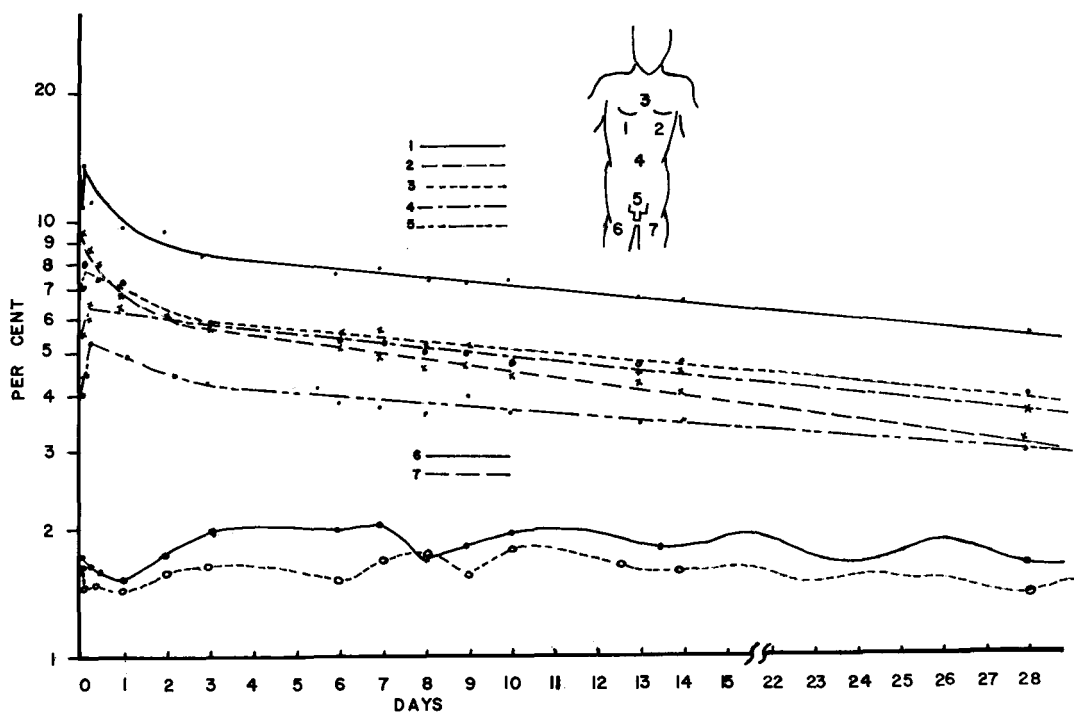
Figure 31.   ^{75}Se-selenomethionine elimination curves over various body areas

In an attempt to quantify the results the counts were compared to that from a one liter plastic flask containing 50 μci ^{75}Se-selenomethionine diluted in one liter water.

CHAPTER III. RESULTS

III-a. <u>The biological half life of</u> ^{75}Se-selenomethionine.

III-a-1. Total body. The counts—corrected for decay and nor-
malized as 1.00 for time zero—were plotted on individual graphs. The
zero time count was 24,000 cpm ranging between 21,000 and 26,000. The
ordinate was the logarithm of the normalized counts, the abscissa—the
time. In 7 out of 9 control subjects the graph resolved into three clear
segments. The general expression of the function is of the type:

$$y = P_1 e^{-\lambda_1 t} + P_2 e^{-\lambda_2 t} + P_3 e^{-\lambda_3 t}$$

The curves of the three patients with chronic pancreatitis resolved
in an identical pattern. The patient with severe pancreatic insufficiency
with high grade diabetes mellitus showed an extremely fast disappearance
of ^{75}Se-selenomethionine from the body.

The curves from all five lymphoma patients resolved only into two
segments, the general function being of the type:

$$y = P_1 e^{-\lambda_1 t} + P_2 e^{-\lambda_2 t}$$

Figures 32a, 32b, 32c and 32d show a typical curve of a normal
subject, a patient with chronic pancreatitis, a malignant lymphoma and the
patient with pancreatic insufficiency and diabetes mellitus, respectively.

As there was no significant difference between the controls and the
pancreatitis subjects, and only one patient with pancreatic insufficiency
associated with diabetes mellitus was counted, the subsequent statistical
analyses were performed on normal controls and lymphoma patients only.

The curve for each subject was fitted by the least square method,
using a DAC-512 computer. Each segment was fitted for a general expression

a

b

c

d
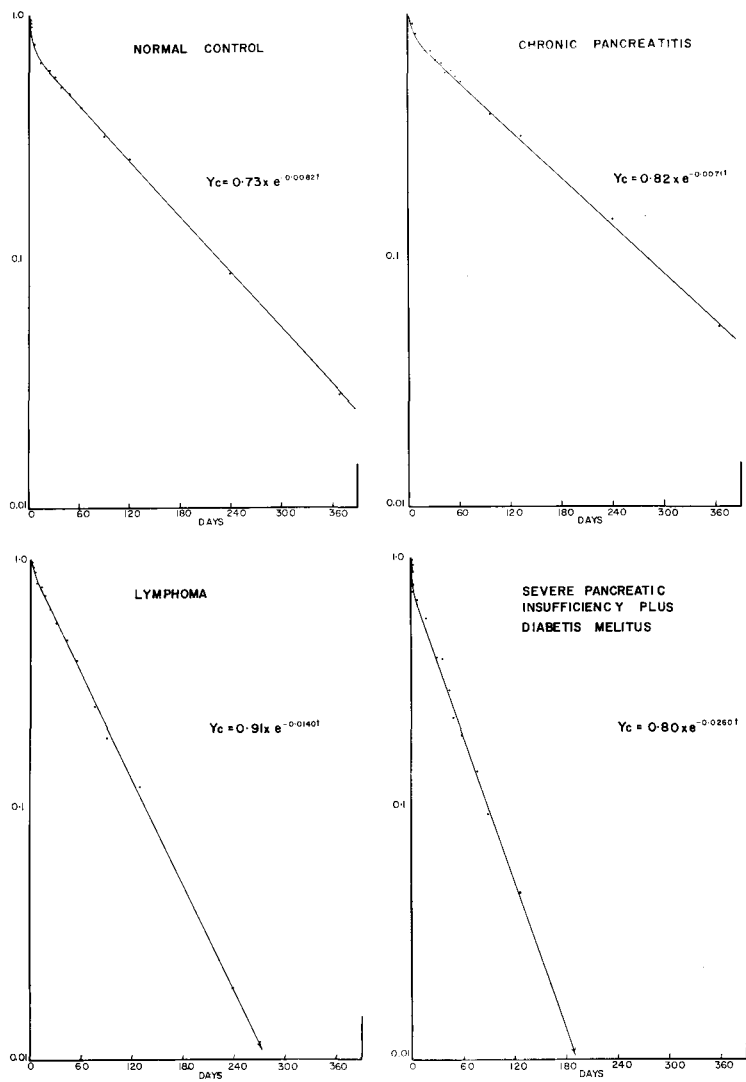
Figure 32. ^{75}Se-selenomethionine total body elimination curves.
(a) Normal; (b) Chronic pancreatitis; (c) Lymphoma;
(d) Severe pancreatic insufficiency and diabetes mellitus.

of the type:

$$\ln P = -\lambda t$$

where P represents the fraction of the administered dose that will be
excreted from the body at a rate. λ is referred to as the excretion
constant. t- is the time, in days, the units of λ are $(days)^{-1}$. P has
no units. The values of P and λ for each segment in each group were aver-
aged and according to these calculated data, the average curves plotted.
The average values corresponding to the various times (t) at which counts
were performed were introduced into the respective graphs. P and λ values
of the averages were calculated and found to be identical to the averages
of the individual P and λ values.

From the λ values, the corresponding half life ($T_{\frac{1}{2}}$) for each seg-
ment may be calculated by the following equation:

$$T_{\frac{1}{2}} = \frac{\ln 2}{\lambda} = \frac{0.6931}{\lambda}$$

The three segments of the control graphs were designated A, B and C
correspondingly. The respective p, and $T_{\frac{1}{2}}$ values: $P_A, \lambda_A, T_A; P_B, \lambda_B,$
T_B and P_C, λ_C, T_C. In the lymphoma patient graphs, segment B was con-
sistently absent.

As mentioned above, the corresponding P- values indicate the fraction
of the administered dose that is excreted at the rate λ. In other words
the fraction P_i of the administered dose will have in the body a biological
half life T_i. Thus, the overall biological half life (T_b) of the total
dose administered will equal the sum of the products $P_i T_i$:

$$T_b = P_A T_A + P_B T_B + P_C T_C$$

$$P_A + P_B + P_C = 1.00$$
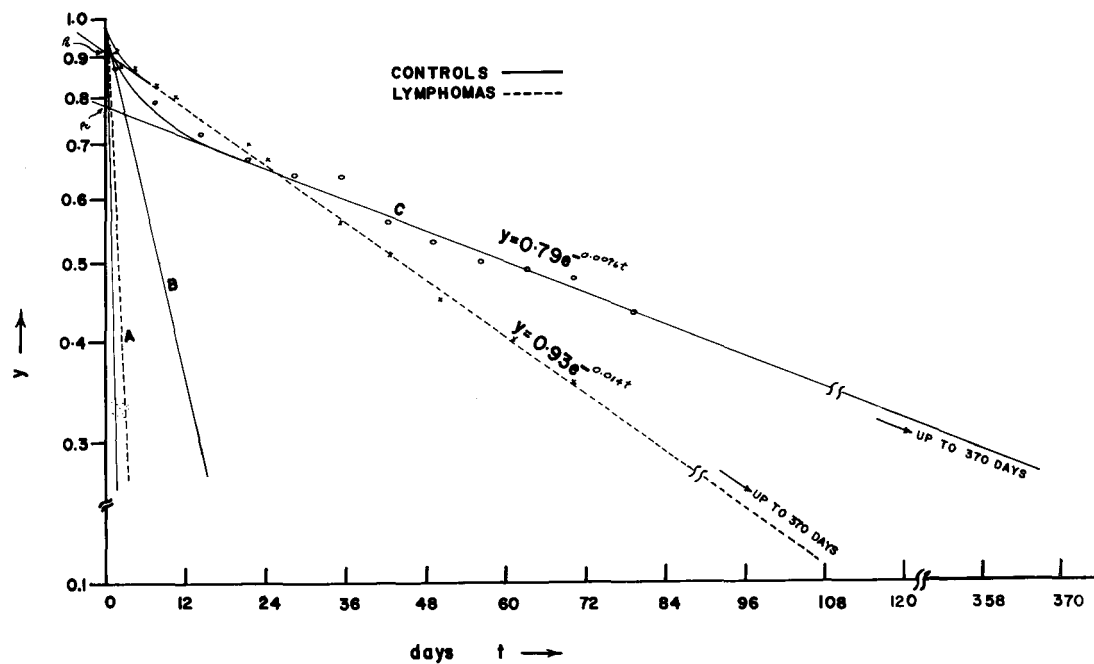
<u>**Figure 33.**</u>   ^{75}Se-selenomethionine elimination curves in normal
controls and lymphomas (average values).

TOTAL BODY ELIMINATION CONSTANTS

	T_A**	P_A	T_B	P_B	T_C	P_C	T_b	T_e
Controls								
J.K.	24.0	0.12	0	0	48	0.88	45	33
M.B.	12.0	0.11	0	0	84	0.78	67	44
E.B.	6.0	0.09	8.0	0.12	92	0.72	72	46
J.S.	4.0	0.175	6.5	0.125	85	0.68	59	40
J.G.	4.0	0.09	6.0	0.12	73	0.77	57	40
E.K.	4.0	0.13	8.0	0.14	123	0.67	84	50
T.K.	4.0	0.125	7.0	0.105	90	0.76	70	46
B.K.	4.0	0.11	18.0	0.11	123	0.77	97	55
E.G.	24.0	0.165	23.0	0.105	102	0.72	76	48
Average	9.5	0.12	8.5	0.09	91	0.76	73	46
S.D.	8.0	0.03	8.0	0.05	36	0.07	21	10
Lymphoma								
E.S.	0	0	0	0	42	1.00	42	31
M.K.	4.0	0.06	0	0	46	0.94	43	32
M.T.	12.0	0.07	0	0	58	0.93	54	37
M.Z.	24.0	0.17	0	0	50	0.86	43	32
H.R.	12.0	0.13	0	0	50	0.90	45	33
Average	10.5	0.08	0	0	49	0.93	45	33
S.D.	9.0	0.03	0	0	6	0.06	8	5
Chr. Panc.								
E.F.	9.0	0.07	8.5	0.11	98	0.82	81	48
W.E.	11.0	0.05	10.0	0.09	76	0.86	66	43
A.R.	10.0	0.06	8.0	0.08	69	0.86	60	40
Average	10.0	0.06	9.0	0.09	81	0.85	69	44
J.D.*)	12.0	0.20	0	0	26	0.80	21	18

*) Pancreatic insufficiency & severe diabetes mellitus.

**) T_A - in hours; all other T's - in days.

TABLE VIII

BIOLOGICAL HALF-LIVES AND DOSE DISAPPEARANCE (AVERAGE VALUES $\pm$ S.D.)

	T_A (hr)	P_A	T_B(days)	P_B	T_C(days)	P_C	(days)$^{-1}$	T_b(days)	T_e(days)
Controls	9.5 ± 8	0.12 ± 0.03	8.5 ± 8	0.09 ± 0.05	91 ± 36	0.79 ± 0.07	0.0076 ± 0.003	73 ± 21	66 ± 10
Lymphomas	10.5 ± 9	0.08 ± 0.03	Absent		49 ± 6	0.93 ± 0.06	0.0140 ± 0.003	45 ± 8	33 ± 5
Significant differences (P values*)	--	--	--	--	< 0.01	< 0.01	< 0.01	< 0.05	< 0.05

TABLE IX

The effective half life (T_e) is a function of both the physical half life (T_p) and the biological half life:

$$\frac{1}{T_e} = \frac{1}{T_p} + \frac{1}{T_b}$$

$$T_e = \frac{T_b \times T_p}{T_b \quad T_p}$$

for ^{75}Se-selenomethionine, $T_p = 120$ days, therefore:

$$T_e = \frac{120 \ T_b}{T_b + 120} \quad (T_e \text{ and } T_b \text{ in days})$$

Table VIII shows the individual data, Table IX summarizes the significant results.

The difference between the corresponding averages of the control data (X_c) and lymphoma data (X_l) were analyzed for significance by the t- test:

$$t = \frac{(N_c + N_1 - 2) \ (\bar{X}_c - \bar{X}_1)}{(\bar{X}_c - X_{ci})^2 + (X_1 - X_{1i})^2} \quad \frac{N_c \ N_1}{N_c + N_1}$$

The corresponding p values are shown in Table IX.

Figure 33 shows the half life curves of the average values of controls and lymphomas.

The results of this experiment may be summarized as follows:

1) The biological half life curve of ^{75}Se-selenomethionine in normal control subjects is resolvable into 3 distinct phases, rapid, inter-mediate and slow, each being characterized by a different excretion rate.

2) In subjects suffering from malignant lymphomas, the intermediate phase

is absent.

3) the slow phase is significantly faster in lymphomas, compared to
controls.

4) Both, the overall biological half life and the effective half life
is significantly shorter in lymphoma patients compared to controls.

5) There appears to be no significant difference regarding the rapid
phase.

6) There appears to be no significant difference between the half life
curve of patients with chronic pancreatitis compared to controls.

7) In a single case of severe pancreatic insufficiency associated with
severe diabetes mellitus, the elimination rate of ^{75}Se-selenomethionine
from the body is abnormally fast.

III-a-2. Half life and tissue distribution in various organs. The
biological half life in various parts of the body was measured by the
technique described in II-e-3. A typical set of curves is shown in fig.
31. The units on the ordinate represents percent per solid angle volume
of the detector system. As this technique of counting was rather crude,
no attempt was made to actually quantify these data. They are however
of qualitative value, as they represent correct half lifes and concentra-
tions in the parts counted, relative to each other.

The organs counted by this method were the liver (1)*, spleen (2)*,
heart (3)*, intestines (4)*, urinary bladder (5)* and skeletal muscle in
the right and left thighs (6,7)*.

---

*-these numbers refer to those in fig. 31.

It appears that among the 7 sites counted, the highest concentration of ^{75}Se-selenomethionine is in the liver. The concentrations in the spleen, heart and intestines are similar. A somewhat lower concentration over the urinary bladder. The skeletal muscle concentration is lower by a factor of about 5. The biological half lifes in the liver, heart, spleen and urinary bladder are similar, about 30 days. In the intestines it is shorter, 17 days. In skeletal muscle, however, there appears to be a very slow release of incorporated ^{75}Se-selenomethionine, unmeasurable over the period observed. A half life of infinity was assumed for this tissue.

The concentration of ^{75}Se-selenomethionine in the organs of the patient who died of bronchogenic carcinoma (II-d-2) was determined. Tissue samples from the organs listed in Table VI were obtained. Where possible the entire organ was weighed. The weight of the organs marked by *) are estimated. The concentrations in some organs of the patient who died of hepatoma are listed in Table X. In the first patient (Table IV), the highest concentration was found to be in the kidney, the lowest in bone. The highest total percent of the administered dose was found to be in the liver, the lowest—0.1% or less—in many organs, mostly of small mass of less than 50 gms.

The data obtained from the lung, are atypical, as the lungs were fibrous and necrotic with large infiltrations of tumor mass. This accounts for the heavy weight and high percentage dose in this organ.

^{75}Se concentration in different organs 52 days following 250 μC ^{75}Se-methionine administration. (Single case, hepatoma.)

Organ	^{75}Se Concentration	Organ Weight	% Administered Dose in Organ
Liver tumor	7.2 X 10^{-3} μC/g ⎫		
Liver	8.1 X 10^{-3} μC/g ⎬ 2400 g ⎫		7.7
Liver	8.2 X 10^{-3} μC/g ⎭		
Kidneys	10.2 X 10^{-3} μC/g	255 g	1.0
Spleen	5.5 X 10^{-3} μC/g	600 g	1.3
Pancreas	1.9 X 10^{-3} μC/g	80 g	< 0.1

TABLE X

III-b. Scanning.

III-b-1. Subtract photoscanning of the pancreas. The results of scanning the model system described above may be visualized in fig. 20. The ^{75}Se-selenomethionine within the inner plastic bottle may be visualized clearly when the ^{198}Au and ^{75}Se-selenomethionine in the outer container are eliminated by subtracting gold from selenium.

In the 25 patients scanned, the pancreas was consistently visualized with the exception of three patients early in the series, while technical improvement in the circuitry was still being made.

Serial scanning indicated continuous accumulation of ^{75}Se-selenomethionine in the pancreas for periods up to seven hours following intravenous administration of labeled selenomethionine. The criteria for accumulation was successively denser pancreatic image with the maintenance of constant scanner control settings and patient-detector geometry (fig. 34). Such accumulation was decreased by a regular lunch but was not affected by substituting a glass of orange juice for lunch.

The principal anatomical variations in the normal pancreas encountered in this study are exemplified by the pistol-shape pancreas, (fig. 35); the pancreas with a large head and small tail, (fig. 21), and the most common variant encountered in this study in which the tail is more massive than the head and a marked attenuation is observed where the pancreas crosses the aorta (fig. 37b). This latter figure also compares the ^{198}Au liver scan (fig. 36), the ^{75}Se-selenomethionine scan (fig. 37a) and the subtract scan which eliminates the liver (fig. 37b).

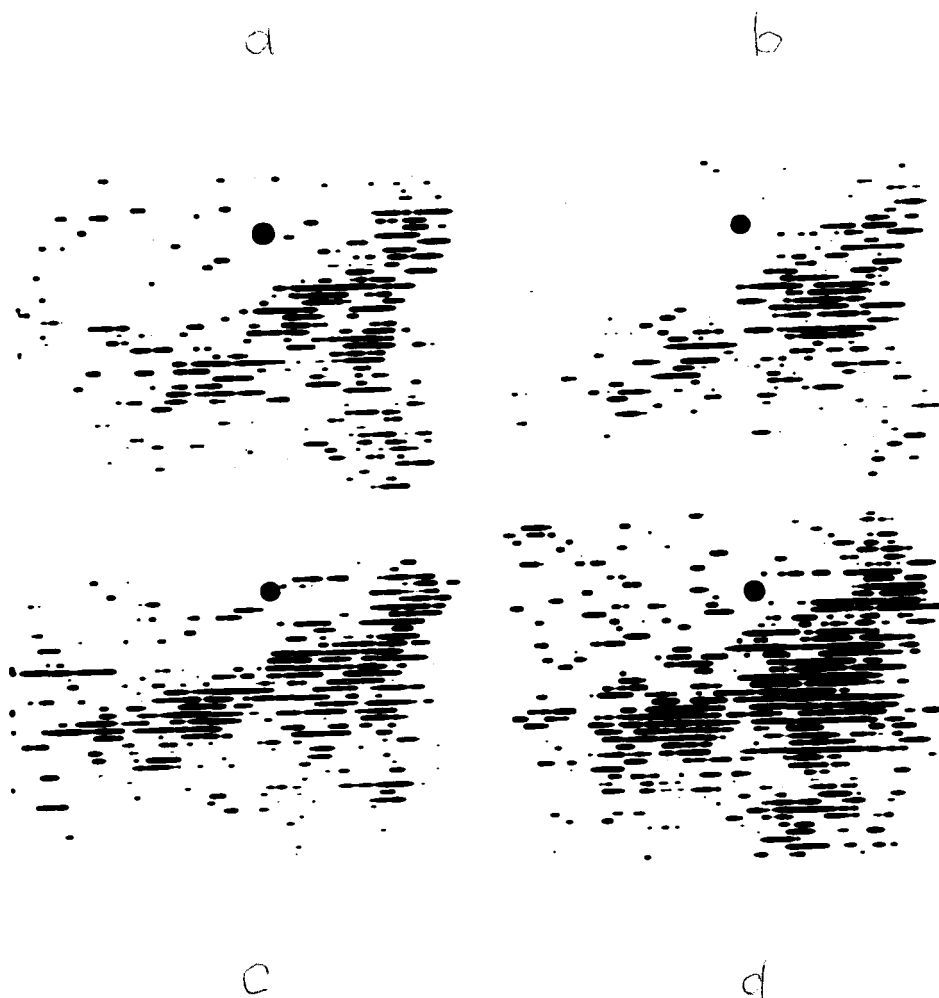Insufficient cases of carcinoma and other pathologies of the pancreas

Figure 34. Pancreatic scan by gold subtract method, showing progressive accumulation of ^{75}Se activity at (a) 30 minutes (b) 2 hours 30 minutes (c) 4 hours 30 minutes, and (d) 6 hours 40 minutes following injection of ^{75}Se-selenomethionine. The subject was a 49 year old male with normal pancreatic function.

Figure 35. Selenomethionine pancreas photoscan by gold subtract method from a 75 year old male subject showing pistol-shape configuration.

Figure 36. Photoscan of the distribution of ^{198}Au in the liver of a 37 year old normal subject.
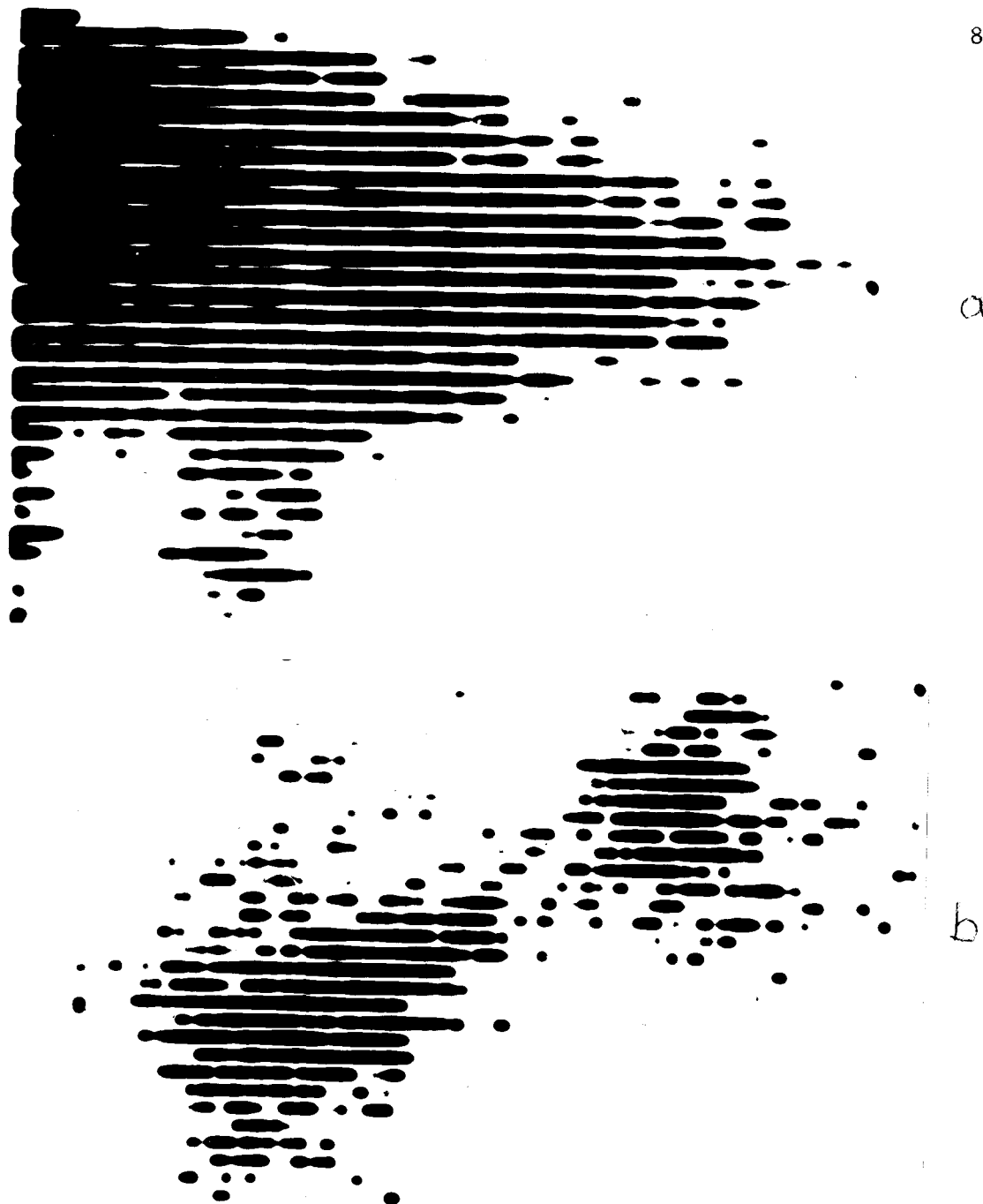
<u>Figure 37.</u> (a) Photoscan showing distribution of ^{75}Se-selenomethionine in the liver and pancreas of the subject in Fig. 36. Note overlap of the two organs. (b) Subtract photoscan of the same subject showing the pancreas without liver interference.

Figure 38. Subtract photoscan of patient with subsequent surgically proven carcinoma of the pancreas.
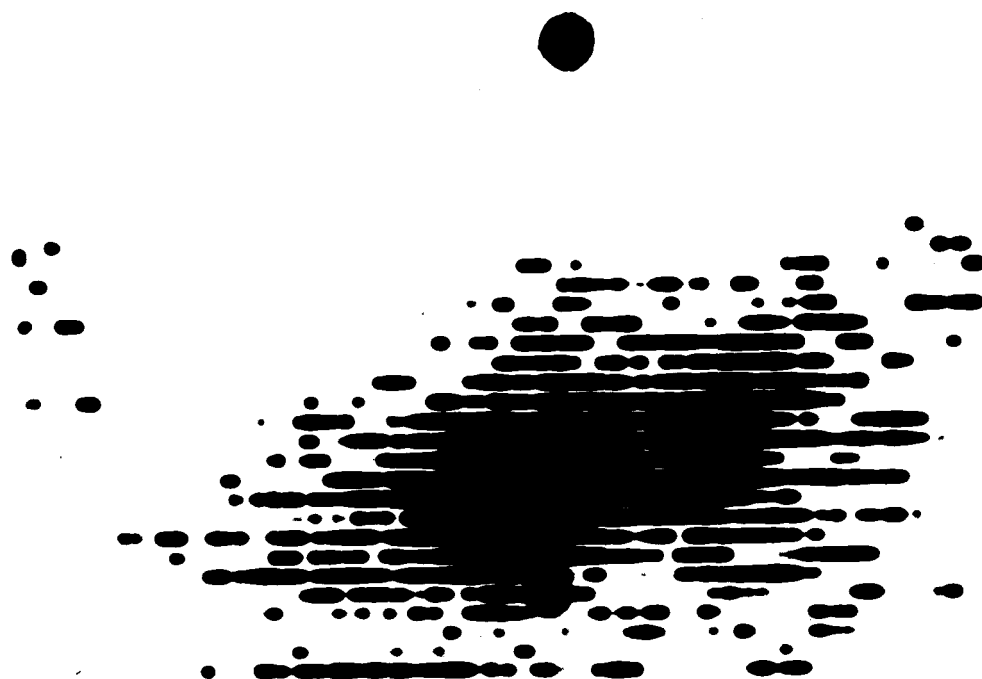
Figure 39. A selenomethionine photoscan using gold subtract method of the pancreas of a 42 year old male patient with chronic pancreatitis. This pancreas was shrunken in size; its length was 10 cm as compared to 15 to 20 cm length seen in normal subjects.

have been completed by this method to make any significant evaluation of

this technique in pancreatic pathology. Two illustrative scans are

shown to indicate the findings in pancreatic disease. Figure 38 shows

the pancreatic scan in carcinoma of the pancreas. The day following the

scan, laparotomy demonstrated that this patient with obstructive jaundice

had virtual destruction of the head of the pancreas and a portion of the

tail by carcinoma. Figure 39 indicates a scan obtained in a patient with

a history of chronic pancreatitis. The pancreas was visualized, but was

markedly shrunken in size. Decreased size was not necessarily an observed

characteristic in other patients with this diagnosis.

III-b-2. Pancreas and liver energy-to-color modulation: Mechanical

display. The correlation of diagnostic results in the 109 patients studied

by this method is summarized in Table VII.

Patients without pancreatic diseases. The pancreas and liver were

consistently visualized in 30 of 36 subjects free of pancreatic and hepatic

disease and no significant defect was seen. Principal anatomic variations

encountered by this method were similar to the above described. These

variations in configuration have been described previously by other

authors (25). Selenium activity exclusive of hepatic and pancreatic was

minimum, and was principally confined to the myocardium (see below). The

spleen was not visualized (fig. 28a).

Carcinoma of the pancreas. The pancreatic scan of 8 of 10 patients

with carcinoma showed "cold" areas in the gland. The spleen was not

visualized, and there was little ^{75}Se-selenomethionine outside of the

pancreas and the liver areas. In one patient with carcinoma of the body

and tail of the pancreas, these areas were devoid of ^{75}Se-selenomethionine but the head appeared normal. In many instances the "cold" areas were diffused, and later anatomical examination revealed replacement of the pancreas in these areas by masses of tumor tissue. In three instances the diagnosis of carcinoma was made in patients in whom barium meal examinations were interpreted as normal by a qualified radiologist. The relative merit of barium meal versus scanning was not accomplished. In one instance the two-color print out revealed cold areas in the liver and pancreas, without ^{198}Au in the spleen or ^{75}Se-selenomethionine in the abdominal field exclusive of the liver and pancreas, which made possible a correct diagnosis of carcinoma of the pancreas with metastases to the liver. In two other cases, scans were interpreted as normal in patients with suggestive x-ray evidence for carcinoma; laparotomy confirmed that the pancreas was normal. Fig. 28b exemplifies a dual color scan of pancreatic carcinoma.

Chronic pancreatitis. In 12 of 19 patients with chronic pancreatitis the scan also differed greatly from those of normal subjects. These patients did not have evidence of liver disease, and splenic uptake of ^{198}Au was absent in every instance, with normal deposition of radiogold throughout the liver. ^{75}Se-selenomethionine activity did not delineate the pancreas because of excessive ^{75}Se-selenomethionine activity in the body exclusive of the liver and pancreas. It has subsequently been determined (by the tape recording method) that the pancreas is discernible in these cases if much greater background erasure is used. This pattern has not been observed in normal subjects, patients with cirrhosis without chronic
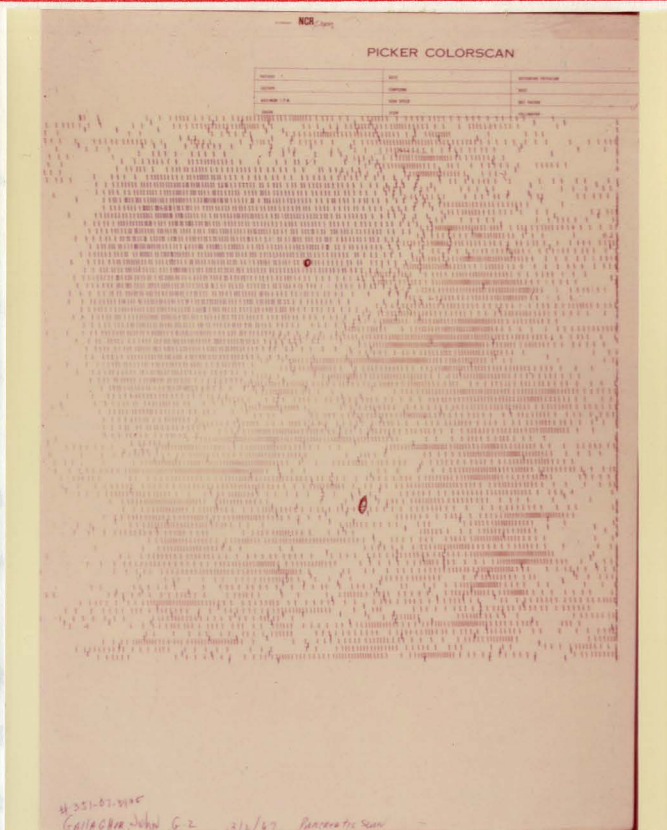
Figure 40. Pancreatic insufficiency visualized by the method described in Fig. 27.
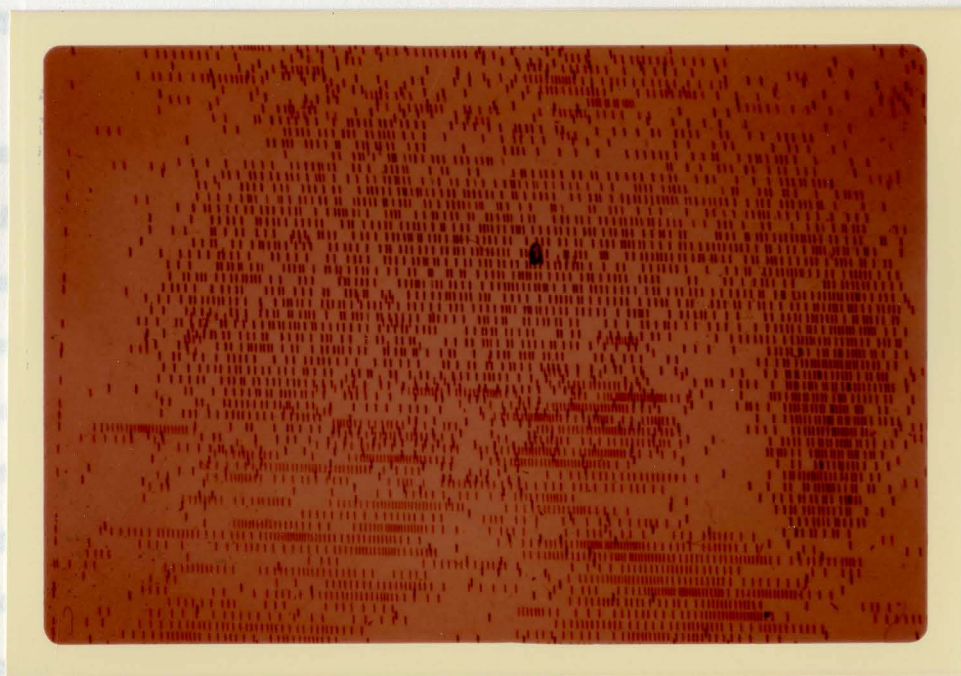

Figure 41. Cirrhosis of the liver visualized by the method described in Fig. 27.

pancreatitis, or in patients with carcinoma of the pancreas. A typical
scan of chronic pancreatitis is illustrated in fig. 40.

Cirrhosis. The scans of 10 of 17 patients with cirrhosis differed
in three significant aspects from those of normal subjects. All showed
patchy distribution in the pancreas, with small, scattered foci of ^{75}Se-
selenomethionine activity. This scattering is probably related to
decrease count rate. In every case but one, the scans also showed
increase ^{198}Au uptake by the spleen (fig. 41).

III-b-3. Pancreas and liver energy-to-color modulation: Tape
recording. The diagnostic advantage of simultaneous scanning and display
of liver and pancreas in separate color using the two color subtraction
technique has been described above.

The tape recording and subsequent cathode ray tube display of the
scans facilitates a significant improvement in the image. The display
of the normal pancreas and liver in blue and red respectively allows
specific and simultaneous delineation of each organ when they are discretely
separated (fig. 42), or when the images overlap (fig. 43). In the later
instance, the area of overlap is seen in white effectively revealing the
boundary of distribution of each isotope in the individual organs. The
effectiveness of the background subtraction in display of the pancreas
is emphasized in figure 44a,b,c and d, in which the liver is displayed at
constant intensity with successive decreased subtraction of background of
the extrahepatic selenomethionine. At low level of suppression the
concentration of ^{75}Se-selenomethionine in the myocardium becomes apparent.
This aspect will be discussed below.
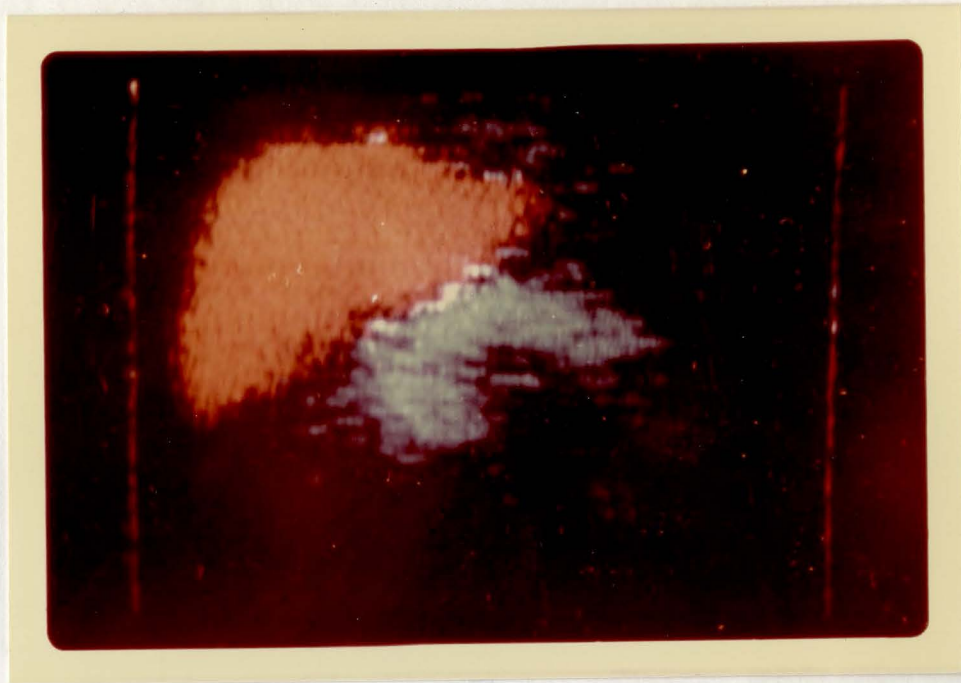
Figure 42. Liver-pancreas scan by the tape method. Both organs are
normal with no overlap.

Figure 43. Normal liver and pancreas, with overlap. White area
represents area of overlap.

a

b

<u>Figure 44.</u> Normal liver and pancreas. (a) No background subtraction,
(b) 30% subtraction, (c) 50% subtraction, (d) 70% subtraction.

c

d

Figure 44.   Normal liver and pancreas.   (a) No background subtraction,
(b) 30% subtraction, (c) 50% subtraction, (d) 70% subtraction.

Background manipulation has been useful in demonstrating cold lesions in the liver which may not be apparent because of saturation effects at low background subtra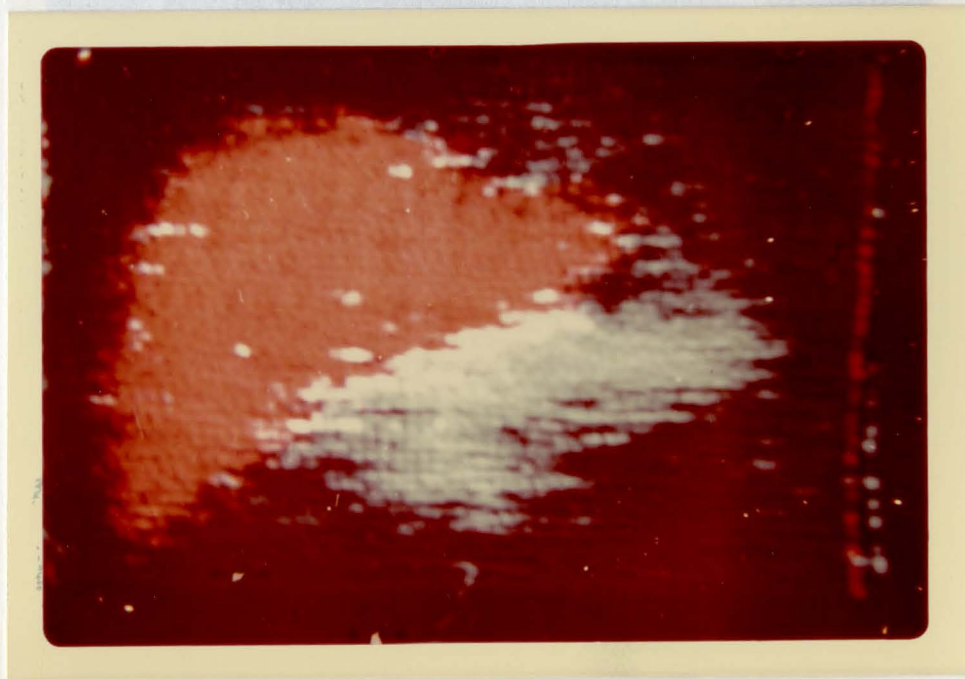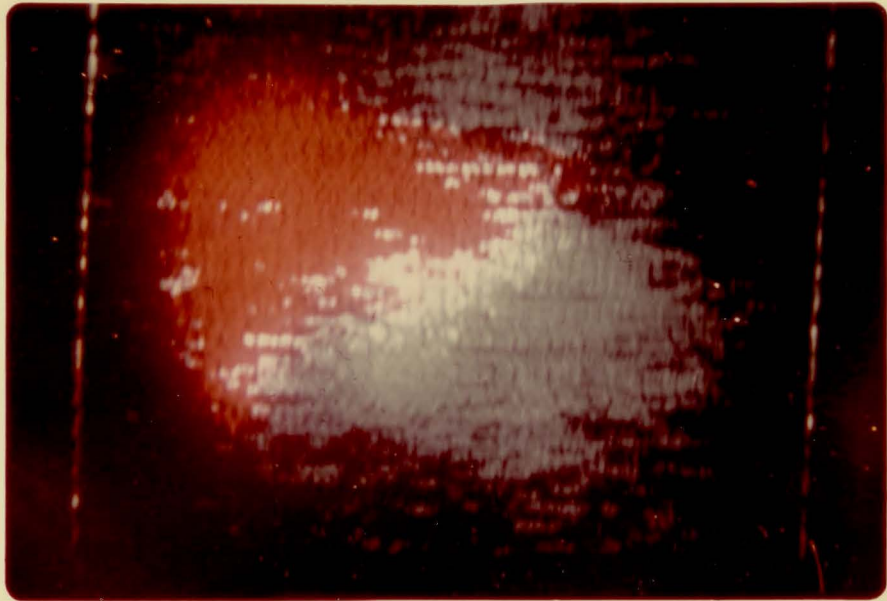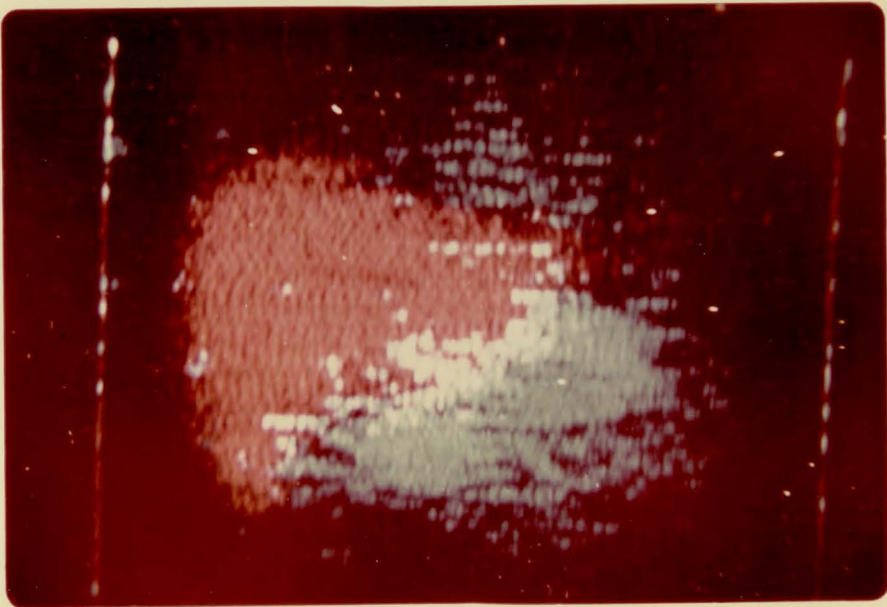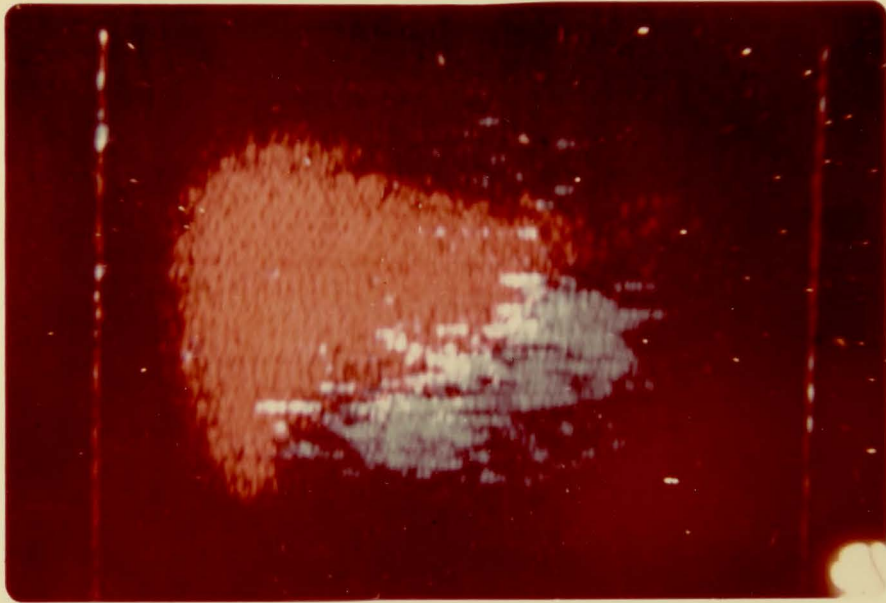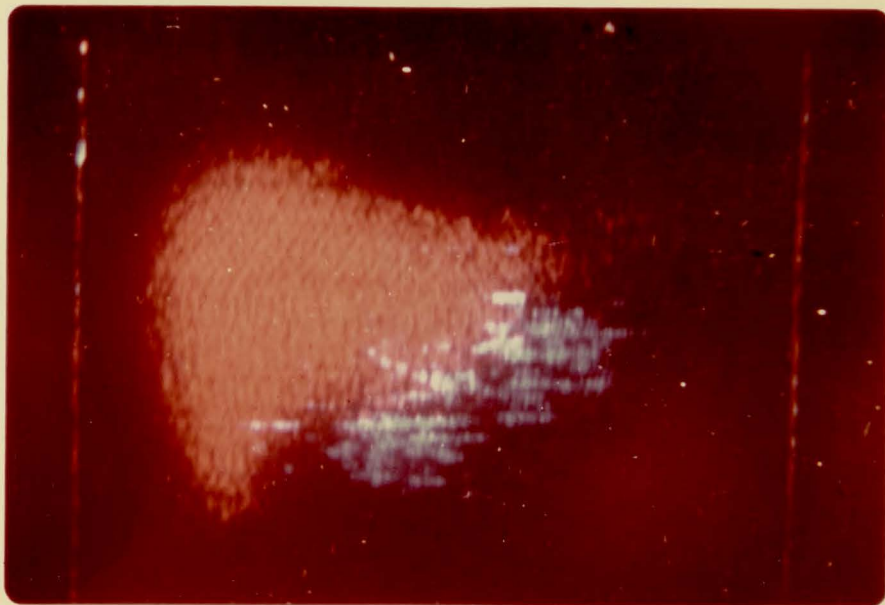ction levels. Display of the tape recorded scan at any desired level of background subtraction for either channel of information is readily accomplished without destruction of any of the information in question. Massive replacement of the liver by metastatic malignancy may occur with no significant localization of ^{75}Se-selenomethionine within the lesions. The pancreas is clearly visualized despite virtually complete overlay of the deformed liver. The enlarged spleen is visualized in red by accumulation of ^{198}Au in figure 45.

The positive visualization of a hepatoma in the right lobe of the liver proven at laparotomy demonstrates massive accumulation of ^{75}Se-selenomethionine (fig. 46). The pancreas was apparently not able to compete with the lesion for the amino acid analogue and is not visualized. A small spleen is seen adjacent to the superior aspect of the left lobe. Using subtraction of gold from selenium activity as previously described, results in separate color visualization of the tumor even if the concentration of ^{75}Se-selenomethionine in the liver and tumor are equal.

Pancreatic defects are well visualized as exemplified by the focal decrease in ^{75}Se-selenomethionine concentration in an individual with verified carcinoma of the pancreas (fig. 47). The focal lesions are quite apparent when compared with scans of the normal pancreas (fig. 42).

Clinical evaluation of this set of results has as yet not been performed.
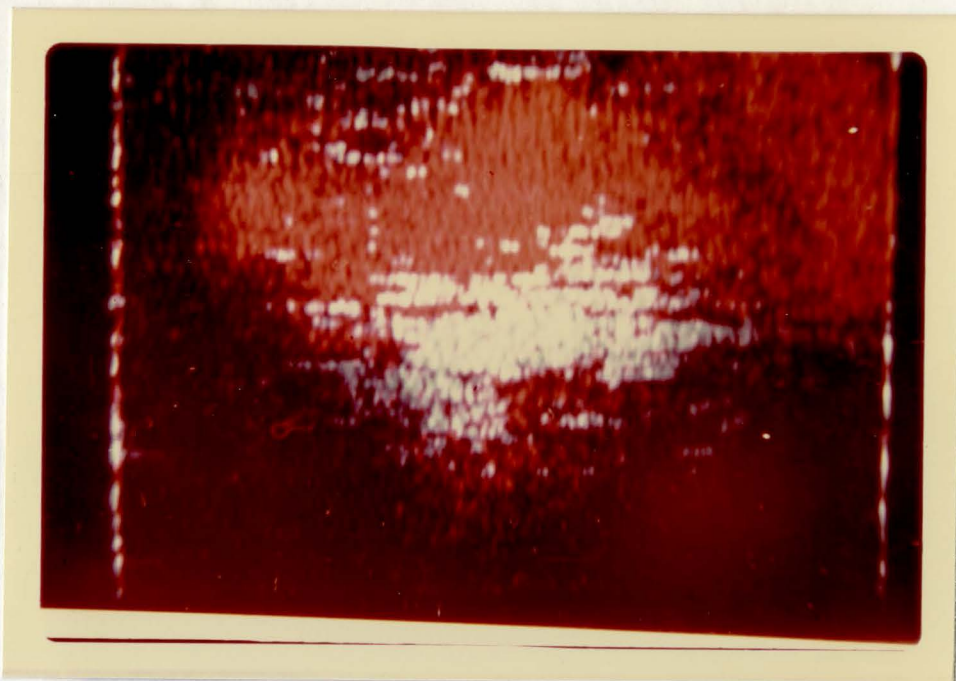
Figure 45. Metastatic involvement of the liver. Despite complete overlap of the liver and pancreas, each organ is clearly visualized and delineated by this method.
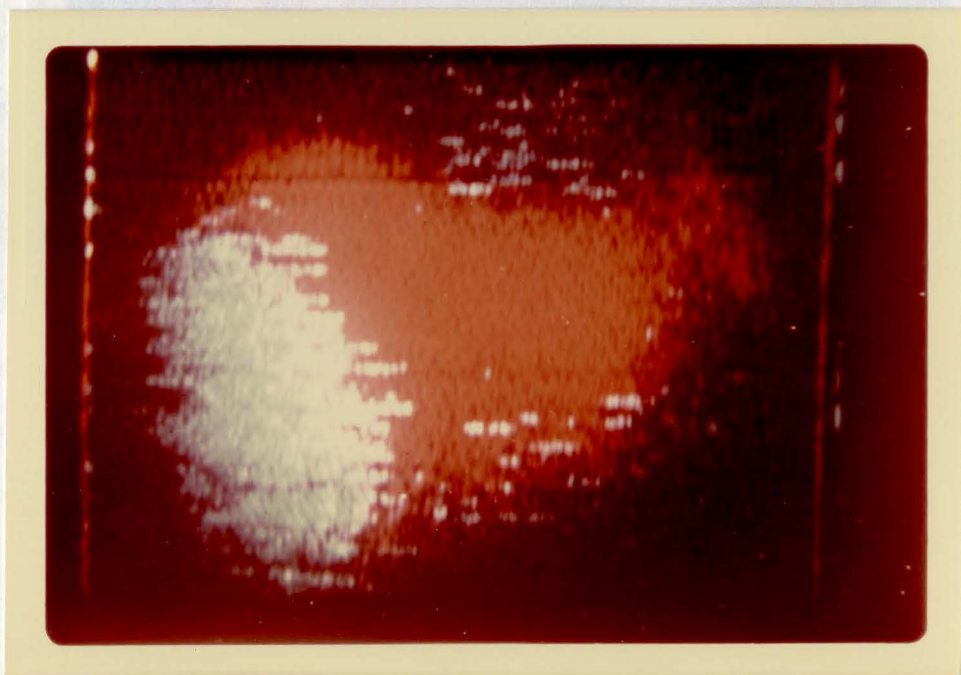

Figure 46. Hepatoma visualized by the tape recording method.

Figure 47. Carcinoma of the pancreas.

III-b-4. Hepatoma. Five patients suffering from hepatoma were scanned. In three of these patients the hepatoma was visualized by a "positive" selenium lesion.

A conventional colloid ^{198}Au scan of the liver shows a "cold" mass in the liver, which may be produced by any space occupying lesion, malignant or benign (fig. 48). The dual color scan, however, shows a "hot" concentration of selenomethionine in the lesion (fig. 49). This was found to be typical of hepatoma.

Fifty-two days after these scans were performed, a necropsy revealed a hepatoma. A massive tumor was found in the liver (fig. 50) precisely at the location revealed by the scan. Tumor cells were spread throughout the entire liver with several nodules of various sizes. Five gram specimens of various organs were obtained and the ^{75}Se-selenomethionine concentration was determined (Table X) and revealed to be equal in both liver and hepatoma at 42 days post administration. No information is available concerning relative concentration at the time of scanning. Assuming equal concentration at the time of scanning, the ^{75}Se-selenomethionine in the hepatoma would still be visualized by this method as ^{198}Au did not concentrate in the tumor allowing the nonsubtracted ^{75}Se-selenomethionine in the hepatoma to be visualized as a separate color. Figure 46 is an example of a hepatoma scan produced by the tape recorder method.

III-b-5. Brain scanning with ^{75}Se-selenomethionine and ^{99m}Technetium. The concentration of ^{75}Se-selenomethionine in the brain following a 250 μci dose of this isotope for pancreatic scanning is sufficient to visualize the
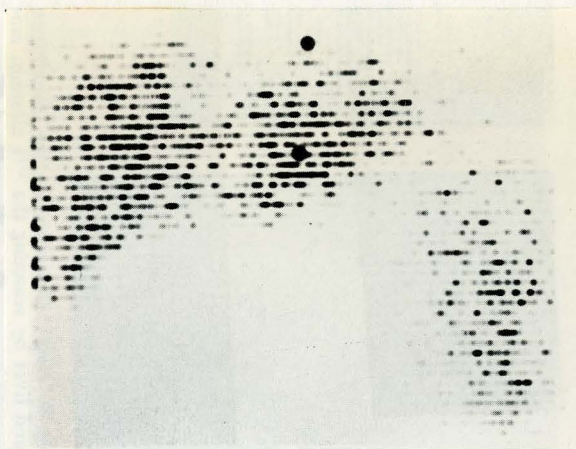
Figure 48. Conventional ^{198}Au liver photoscan, revealing "cold" spot, indicative of a space occupying lesion.

Figure 49. Two-color subtract scan of same patient showing concentration of ^{75}Se in "cold" spot (figure identical to #26).

Figure 50. The patient's liver at necropsy, revealing a large hepatoma at the site of the "cold" spot.

brain by scanning (fig. 51). The accessory structures of the head are not seen. The concentration of ^{75}Se-selenomethionine activity equilibrates within ten minutes of intravenous injection and remains at a significant concentration within the brain for at least several hours. When a simultaneous scan of ^{99m}Technetium and ^{75}Se-selenomethionine are attempted the gamma energy of the two isotopes may be discriminated, stored in separate magnetic tape channels and each displayed on Polaroid film as described above. In the example shown (fig. 52), the ^{99m}Tc and ^{75}Se-selenomethionine are displayed in yellow and blue respectively. The overlay of these two colors produces a display of the lesion in white. The usefulness of this methodology in diagnosing and discriminating various brain lesions remains to be explored. It would appear of use in differentiating ^{99m}Tc containing normal vasculature from brain lesions.

III-b-6. Myocardial scanning with ^{75}Se-selenomethionine. As seen in Table VI, the relative myocardium: skeletal muscle concentration of ^{75}Se-selenomethionine is 4:1. The differential is probably greater at lesser intervals following intravenous injection. The high concentration of ^{75}Se-selenomethionine in the myocardium has permitted visualization of the myocardium by dual channel scintiscanning. An example of such a scan (fig. 53) differentiates the liver from the myocardium by dual channel subtraction. The tip of the left lobe of the liver and the myocardium are plainly visualized. The cavity of the right heart may be seen. A direct comparison with ^{86}Rb and ^{131}Cs scans of the myocardium has not been made but the quality of the scans obtained with ^{75}Se-selenomethionine
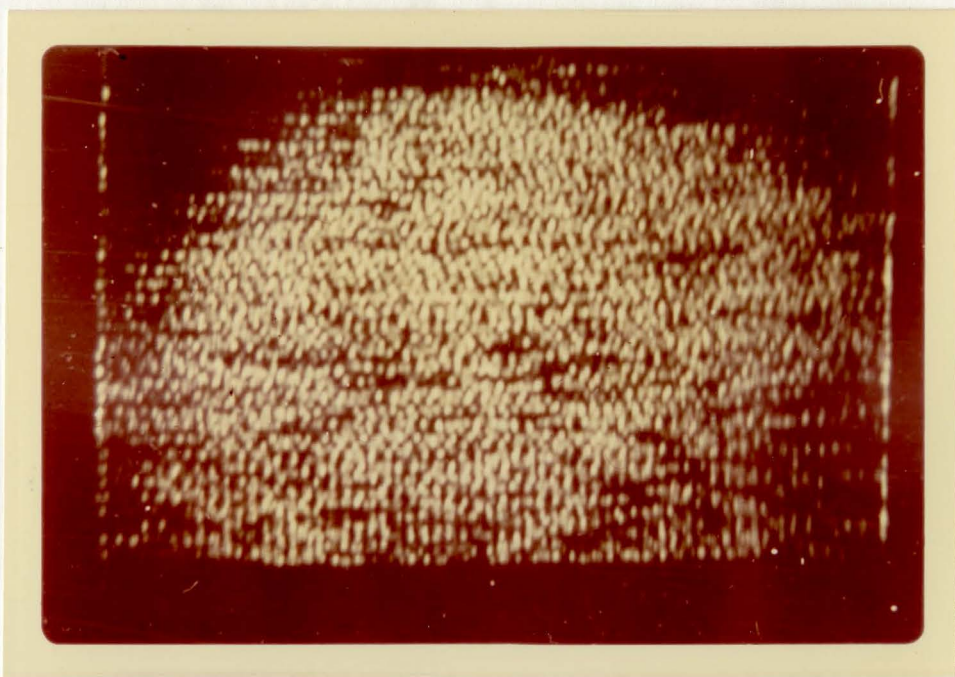
Figure 51. Normal brain distribution of ^{75}Se-selenomethionine.
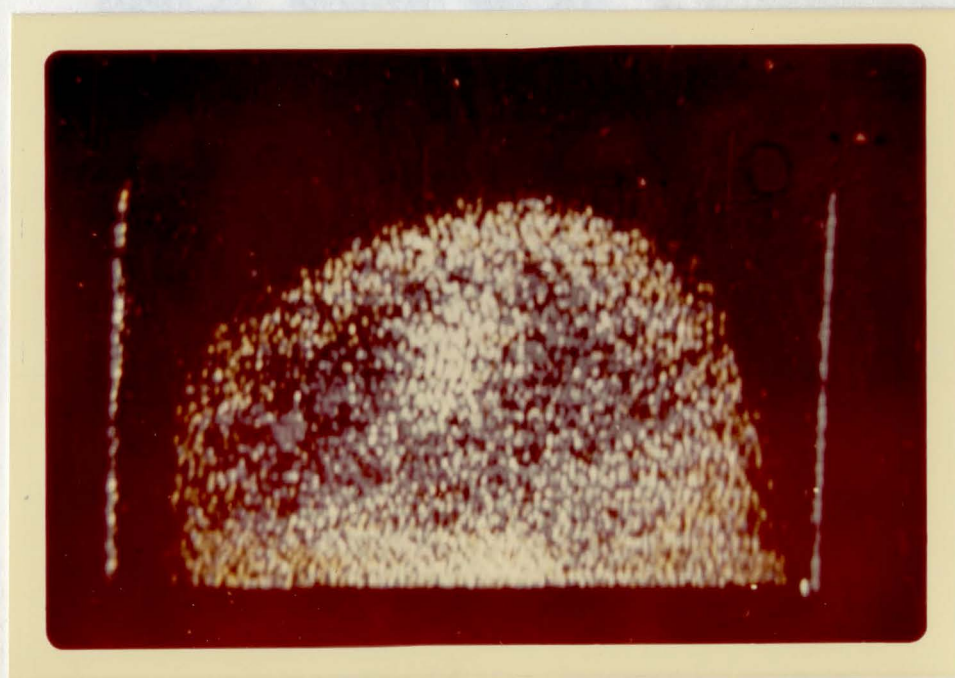
Figure 52. Brain lesion visualized by ^{99m}Tc and ^{75}Se dual isotope scan. Note lesion in different color (white) than normal brain tissue (blue) or normal accessory scalp structure (yellow).

Figure 53. Myocardial scan with ^{75}Se-selenomethionine.
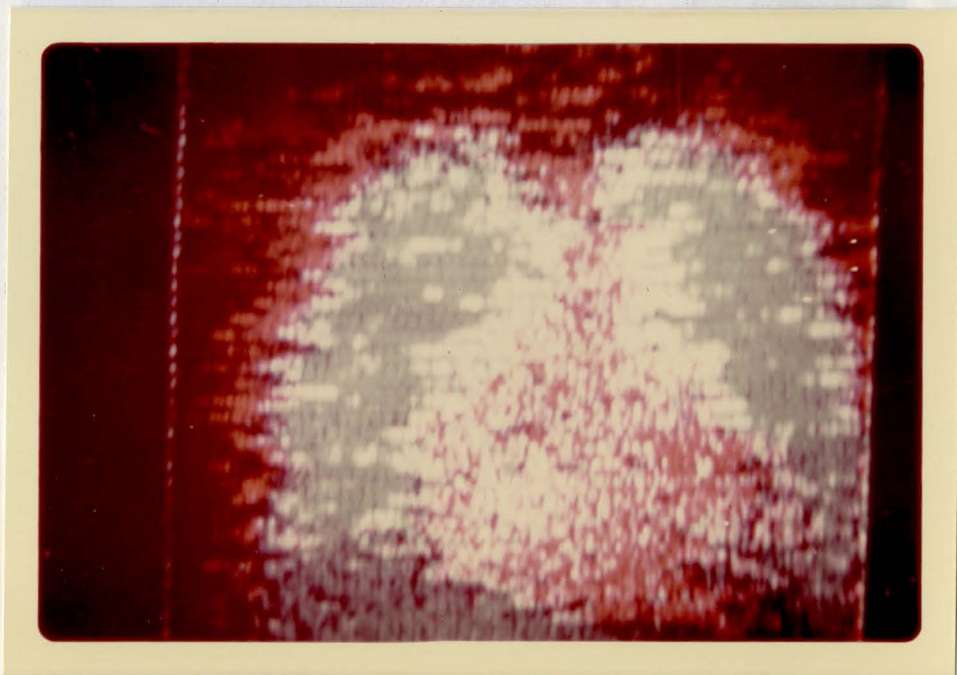
a

Figure 54. Combination chest scan with ^{75}Se-selenomethionine, ^{131}I-macro-aggregated serum albumin and R^{131}ISA. (a) Lungs in blue, myocardium in red and heart blood pool in white. (b) Myocardium (blue). (c) Lungs, blood pool in the ventricles and top of the liver (red).
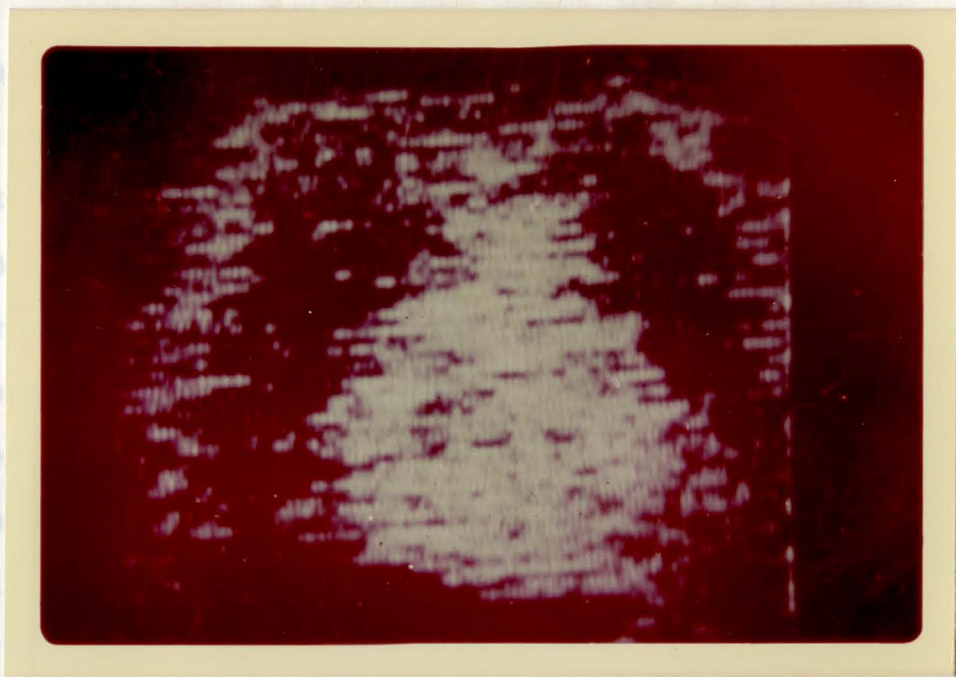
b
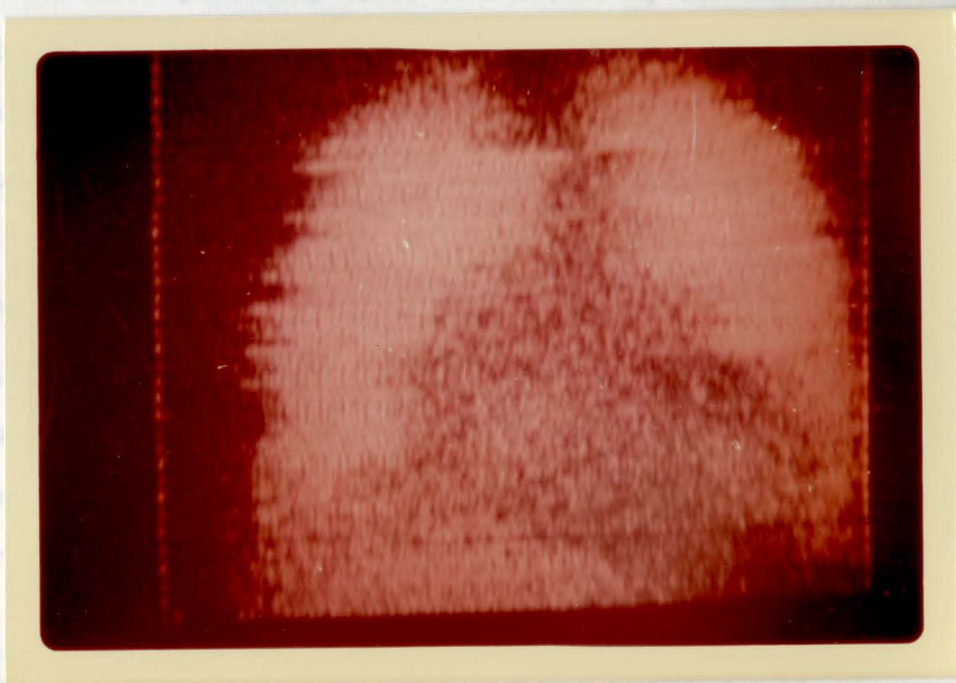
c

Figure 54. Combination chest scan with ^{75}Se-selenomethionine, ^{131}I-macro-aggregated serum albumin and R^{131}ISA. (a) Lungs in blue, myocardium in red and heart blood pool in white. (b) Myocardium (blue). (c) Lungs, blood pool in the ventricles and top of the liver (red).

appear superior to the published scans using other isotopes (82,83).

A specific application of this method is demonstrated in fig. 54. A patient whose chest x-ray showed an enlarged shadow of the heart was scanned to determine whether this shadow represents an enlarged heart or a pericardial effusion. The patient was given 250 μci ^{75}Se-selenomethionine intravenously. One hour later 100 μci ^{131}I-iodinated serum albumin and ^{131}I-macroaggregated serum albumin were administered intravenously to the patient. Ten minutes later the scan was performed. Fig. 54a shows the scan.

The selenomethionine distribution is displayed in red, indicating that the entire interpulmonary space is occupied by the heart. The lungs are displayed in blue. The white and blue areas overlapping with red indicate the blood pools in the right and left ventricles. Fig. 54b shows the myocardial scan, fig. 54c the lungs and the blood in the ventricles.

III-c. Dosimetry.

III-c-1. Total body irradiation. The dosimetric calculations of a radioactive material uniformly distributed in the body or a specific organ, may be carried out by the Quimby-Marinelli formula (84).

The dose due to β-radiation, D_β:

(A) $D_\beta = 73.8 \ E \ CT_e$ rads/μci - upon complete disintegration.

The dose due to γ-radiation, D_γ:

(B) $D_\gamma = 0.0346 \ \Gamma g CT_e$ rads/μci - upon complete disintegration

where:

$$\bar{E}_\beta \quad = \text{average } \beta\text{-ray energy (Mev)}$$

$$C \quad = \text{concentration } (\mu ci/gm \quad)$$

$$T_e \quad = \text{effective half life (days)}$$

$$\Gamma \quad = \text{gamma ray constant } (\frac{cm^2 \cdot rad}{mc \cdot hr})$$

$$g \quad = \text{geometric factor (function of organ size)}$$

For a 70 kg normal male, the constants used in the above equations are as follows:

$$\bar{E} \quad = 0.0105 \text{ Mev (7)}$$

$$T_e \quad = 46 \text{ days (III-a-1)}$$

$$C \quad = \frac{1 \ \mu ci}{70,000 \ gm}$$

$$\Gamma \quad = 2.0 \ \frac{cm^2 - rad}{mc - hr} \text{ (7)}$$

$$g \quad = 126$$

Substituting these values in equation A and B, the result is:

$$(A') \qquad D_\beta \ = \frac{73.8 \times 0.0105 \times 46}{70,000} \ = 0.5 mrad/\mu ci$$

$$(B') \qquad D_\gamma \ = \frac{0.0346 \times 2.0 \times 126 \times 46}{70,000} = 6.0 mrad/\mu ci$$

For a tracer dose of 250 μci, the total body radiation dose from both β and rays is:

$$(C) \qquad D_{\beta+\gamma} \ = 6.5 \times 250 = 1,625 mrads.$$

III-c-2. Radiation dose to individual organs. As mentioned, equations A and B apply to individual organs as well as to the total body dose. The

constant used for the calculation of the dose for individual organs are shown in Table VI as well as the calculated doses. The total body dose of 1.625 rads for 250 μci has to be added to each individual organ dose.

The geometric factor g for each organ was calculated by the following method (84):

The total mass (weight) of the organ is assumed to be shaped as a sphere. The radius R of this sphere is calculated. g is obtained by:

$$g = 3\ R\overline{\pi}\ \ (R \leq 10cm)$$

$$g = 4\ R\overline{\pi}\ \ (R > 10cm)$$

The pancreas receives an additional radiation dose to that shown in Table VI, due to an initially high concentration of selenomethionine. It has been shown that 7% of the administered dose concentrate initially in the pancreas, before being secreted. These 7% have a half life of 24 hours (10). This fraction would account for an additional 0.46 rads/250 μci to the pancreas.

Disregarding the radiation dose to the lung for reasons explained above (III-a-2), the organ that receives the highest radiation dose is the liver.

The 72 hours tissue concentrations have been taken as initial concentrations for dosimetry purpose. In fig. 31 it is seen that by this time, the excretion ratio has stabilized and continues exponentially.

CHAPTER IV. DISCUSSION

IV-a. Half life studies.

The biologic interpretation of the 3 phases observed in the total body half life curves of normal subjects may be relevant to previously published data based on In Vitro studies (11,12,13,14). Phase A (T_A = 9.5 hours) may be the elimination of unbound or nonpeptide bound ^{75}Se-selenomethionine as well as relationship to the pancreatic-enteric recycling of ^{75}Se-selenomethionine.

Phase B (T_B = 8.5 days) has an excretion rate of the same order of magnitude as the half-time of serum protein and may represent incorporation in the relatively rapid metabolizing protein pool, although no specific identification of an incorporating protein has been accomplished.

Phase C (T_C = 91 days) may represent incorporation in red cells, structural proteins and other stable protein moieties. From the data obtained by directional counting it would appear that incorporation into skeletal muscle proteins is a significant contribution to this phase. This phase may also represent re-utilization of recycling ^{75}Se-selenomethionine (11,20).

In the present study, the biological half life in man was directly measured for the first time. It is so far the only study of this type. The result - 73 days - is longer by a factor of 3 than the shortest estimated biological half life published (23,24) and shorter by a factor of 2 than the longest half life suggested (30). The previously published values were based on estimation from data obtained in animals. The present results prove once again, that such practice is inappropriate and should

be avoided whenever possible.

The biological half life in lymphoma patients has been shown to be significantly different from normal subjects quantitatively (slower) and qualitatively (2 phases compared to 3). ^{75}Se-selenomethionine has been shown to be an adequate index for protein synthesis and metabolism by many authors (31-37). Therefore it would appear that the present data indicate a significant impairment of protein synthesis and metabolism in lymphoma patients. Although it would be premature to interpret the absence of phase B in lymphoma patients as an indication of altered serum protein synthesis and degradation, this fact should still be of considerable pathophysiological significance. It remains for future research on this subject to establish whether there actually is a connection between the ^{75}Se-selenomethionine curves and protein metabolism in lymphoma patients and if so is it primary or secondary to the disease. As mentioned before, none of the patients in the group tested had any chemotherapy with anti-metabolites throughout the duration of the experiment.

In the case of severe diabetes, a very rapid excretion rate was measured. This fact may be attributed to the lack of insulin. It is well known that amino acid incorporation into protein is impaired in diabetic patients (85,86,87). This result however, needs to be verified in an experiment where a statistically significant group of patients will be studied. The single case is not presented as a conclusive result, but rather as an observation indicating that further research may be of considerable value.

The organ distribution studies in man presented here are based on a single case, and not on a normal subject, but a patient suffering from bronchogenic carcinoma. Still, this presents the best human data available to date. Animal studies were performed (10,15,17,18), but it would appear that the distribution and concentration of selenomethionine in a normal man are more closely related to that observed in a sick man than to that observed in a normal animal. The most extensive results obtained from animal studies were published by Anghileri and Marques (17). The only similarity between these results and the present information obtained from men, is that in both species the highest concentration is in the liver and kidneys and that the half life in skeletal muscle approaches infinity.

The only organs with malignant involvements in the subject studied in the present work were the lungs and several metastatic lymph nodes. A large mediastinal tumor mass was found and fibrous infiltrations, necrosis and edema in the lungs. This accounts for the twice the normal weight of the lungs. The concentration in the tumor tissue and the malignant involved organs appeared to be of the same order - about 0.35%/100 gr of tissue.

The organs and tissues are arranged in Table VI in a descending order according to the ^{75}Se-selenomethionine concentration. This order parallels roughly the order of protein synthetic metabolic activity of the organs. It therefore is possible that the concentration may serve as an index of metabolic activity. If we arbitrarily chose the relative

concentration index of 1.00 being equal to a concentration of 0.25%/100 gr of tissue, the liver index would be 7.2 compared to an index of 0.16 for bone. Whether this actually is the case remains to be established in future research.

It is evident from the data, that the concentration in cardiac muscle is 4 times that of skeletal muscle of the legs. Although not proven this may be due to the higher rate of activity of the cardiac muscle, which functions rhythmically, and in an involuntary manner compared to the skeletal muscle. This may also account for the 2.5:1.0 concentration found in the diaphragm compared to skeletal muscle.

The total body radiation dose of 1.625 rads per 250 μci administered intravenously is appreciable, but still within safe limits. This is approximately equal to the dose obtained from a gastrointestinal x-ray series examination, which is 1.4 roentgens (89). The organ doses too are of the same order as delivered by equivalent x-ray examinations. The kidney dose from kidney x-rays is 2 roentgens per exposure and from gallbladder radiography the dose is 2.5 roentgens per exposure to the liver (88). Compared to other radioisotope studies, the liver dose delivered by 0.5 μci ^{60}Co-cyanocobalamine for the Schilling test is 22.0 rads (89). The kidney dose from 150 μci ^{203}Hg-chlonerodrin for kidney scanning is 9.0 rads (89). The present results show doses of 5.3 rads to the liver and 3.85 to the kidney from 250 uci ^{75}Se-selenomethionine. These results indicate that a dose of 250 μci ^{75}Se-selenomethionine is a safe dose, well within the range of other established radiological and radioisotopical procedures.

IV-b. <u>Scanning</u>.

Various investigators have reported on ^{75}Se-selenomethionine as

a diagnostic agent in scanning the pancreas. Due to variable criteria

of evaluation of scans and diagnostic methodology, comparison between

series is probably not very meaningful. Burke and Goldstein (90) made

a correct diagnosis of carcinoma of the pancreas in 3 of 4 cases proven

by surgery and diagnosed 2 cases of pancreatic insufficiency. Haynie

et al (91) evaluated 15 normal subjects, interpreting 12 as normal, 1 as

abnormal and 2 as equivocal; 11 patients with carcinoma of the pancreas,

interpreting one as normal, 7 as abnormal and 3 as equivocal; and 11

patients with chronic pancreatitis, one as normal, 8 as abnormal and

2 as equivocal. Sodee (92) made the correct diagnosis in 5 of 6 patients

with carcinoma of the pancreas. Burdine and Haynie (93) reported scan

interpretation in 29 patients with suspected pancreatic disease. Fourteen

had normal scans; 10 patients had "focal areas" in the pancreas, of whom

6 were found to have carcinoma of the pancreas by pathological examina-

tion, and the remaining 4 were not diagnosed. One patient was interpreted

as having chronic pancreatitis and in 4 others liver interfered with the

pancreatic scan. Brown et al evaluated 80 pancreatic scans of which 37

were interpreted as normal, 39 as abnormal and 4 as technically unsatis-

factory. The normal scans included 33 normals, 2 pancreatitis and 1 tumor;

the abnormal scans included 6 normals, 16 pancreatitis and 13 tumors. It

must be emphasized that in contrast to the above studies this investigation

deals with diagnostic categorization into 4 classes: normal, carcinoma

of the pancreas, pancreatic insufficiency and cirrhosis. The pancreatic

lesion must be of sufficient size to permit resolution by the collimation and the counting statistics of the scanning system employed. Small lesions of less than 2 cm circumference would not be visualized by most scanning devices. The lesions reported by this technique are presumably examples of relatively massive replacement. Reference to lesion size includes secondary effect due to occlusion of pancreatic ducts.

Diagnosis of pancreatic disease by ^{75}Se-selenomethionine scanning is atraumatic, the procedure can be tolerated by the most cachectic or gravely ill patient. The present data indicates that dual isotope scan may be helpful in diagnosing carcinoma of the pancreas. Particularly in cases of cancer in the body and tail, scanning may demonstrate suspicious areas which are not visualized by conventional barium meal examinations.

Further investigation is indicated to more precisely determine the relationship of cirrhosis to the apparent decreased pancreatic uptake of ^{75}Se-selenomethionine in this disease as compared to normals. The subtraction technique employed is not a significant factor in this observation as the decrease is independent of liver-pancreas overlap.

Colloidal ^{198}Au uptake by the spleen may be a marker which will help to prevent erroneous diagnoses of carcinoma of the pancreas in patients with cirrhosis.

When cirrhosis is not present (94), the opportunity to detect hepatic metastases by the simultaneous hepatic scan is of clear advantage, giving

important information without the necessity of two separate examinations.

These data also indicate that the energy-color modulation technique can support or suggest a diagnosis of chronic pancreatitis. The diffuse appearance of ^{75}Se-selenomethionine on these scans gives an appearance which was not seen in patients with carcinoma.

Improvement of the method by tape recording the two channels of information as described above, permits great improvement of the quality of the image. This technique permits multiple image production at various channel ratios. Evaluation of pancreatic disease by this improved method has as yet not been completed.

The myocardial scans produced by the tape recording technique are technically superior to any scans published, which have been done using other isotopes and conventional techniques. The mechanism of the rather selective uptake of ^{75}Se-selenomethionine by the myocardium is not well understood. A possible explanation has been offered in the discussion on the organ concentration studies. A clinical evaluation of this application of ^{75}Se-selenomethionine and the scanning techniques developed has as yet not been performed.

Neither has the selenium-technetium brain scan been clinically evaluated. The advantage of this technique is obvious, as it permits discrimination between intracerebral and extracerebral lesions in the head, which cannot be accomplished by use of ^{99m}Technetium pertechnetate or any other scanning agent alone.

SUMMARY

(1) A scanning system has been developed which permits:

    (a) The subtraction of the radiation of one isotope from that of another. This permitted for the first time the visualization of the pancreas without the liver interference, improving this technique significantly.

    (b) The display of the simultaneous distribution of two isotopes in different colors for each isotope.

    (c) Tape recording and color display of the scanning information, permitting "rescanning" at optimal settings.

(2) One hundred and nine pancreatic scans of the 220 patients scanned by this method were clinically evaluated. These scans were performed by the method described in (b) above. It was found that a high degree of accuracy in the diagnosis of pancreatic carcinoma was obtained. There are indications of a distinct pattern for the differential diagnosis of chronic pancreatitis and cirrhosis of the liver.

(3) The use of ^{75}Se-selenomethionine and this system yields myocardial scans superior in quality compared to any other method to date.

(4) ^{75}Se-selenomethionine and ^{99m}Tc-pertechnetate used simultaneously for brain scanning permit the differentiation between intracerebral and extracerebral lesions observed by a technetium brain scan.

(5) Three out of 5 hepatomas show "positive" ^{75}Se-selenomethionine distribution in these tumors in scans done with colloid ^{198}Au and

^{75}Se-selenomethionine.

(6) The biological half life of ^{75}Se-selenomethionine in man has been determined. It has been shown, in normal males, to be composed of three phases: A- rapid, B- intermediate, C- slow. The combined biological half life was 73 days.

(7) In patients with malignant lymphomas, the biological half life is composed of 2 phases only, phase B being absent and the combined biological half life being significantly shorter—45 days. It is proposed that this difference is due to impaired protein synthesis and metabolism in patients suffering from malignant lymphomas.

(8) No significant difference was found between the biological half life of ^{75}Se-selenomethionine in patients with chronic pancreatitis and normal subjects.

(9) Tissue distribution and concentration studies have been carried out in a patient who expired 72 hours following the administration of 250 μci ^{75}Se-selenomethionine. It is suggested that the concentration pattern parallels that of protein synthesis metabolic activity of the various tissues and organs.

(10) Based on these results the total body radiation dose and that to individual organs, resulting from the intravenous administration of 250 μci to be of the same order as doses resulting from other presently employed radiological and radioisotopical diagnostic procedures.

REFERENCES

1. Kent, C. V. and Cork, J. M.: Selenium[75].
   Phys. Rev. 61:389-390, 1942.

2. Hopkins, H. H., Jr.: Spallation products of arsenic with 190 Mev deutrons.
   Phys. Rev. 77:717-718, 1950.

3. Cork, J. M., Rutledge, W. C., Branyan, C. E., Stoddard, A. E.:
   Energy levels associated with Se[75].
   Phys. Rev. 79:889, 1950.

4. Jensen, E. N., Jackson, L., Martin, O. S., Hughes, F. J., Pratt, W. W.:
   Radiations from selenium[75].
   Phys. Rev. 90:557-563, 1953.

5. Schardt, A. W. and Welner, J. P.: Decay scheme of Se[75] and Ga[75].
   Phys. Rev. 93:916, 1954.

6. Dzhelepov, B. S. and Peker, L. K.: Decay Schemes of Radioactive Nuclei.
   Page 177, Pergamon Press, 1961.

7. The Radiochemical Manual, Part 1, pages 54-55.
   Publ.: The Radiochemical Centre, Amershom, England, 1962.

8. Painter, E. P.: A synthesis of selenium analogs of dl-methionine and dl-homocystine.
   J. Am. Chem. Soc. 69:232-234, 1947.

9. Blau, M.: Biosynthesis of Se[75]-selenomethionine and Se[75]-selenocystine.
   Biochim. biophys. Acta, 49:389-390, 1961.

10. Blau, M. and Manske, R. F.: The pancreas specificity of Se[75]-selenomethionine.
    J. Nucl. Med. 4:231-233, 1963.

11. Oldendorf, W. H. and Kitano, M.: Selenomethionine reappearance in blood following intravenous injection.
    J. Nucl. Med. 4:231-233, 1963.

12. Penner, J. A.: Seleno-methionine incorporation into plasma proteins.
    Clin. Res. 12:277, 1964.

13. Awad, H. K., Potchen, E. J., Adelstein, J. and Dealy, J. B.:
    [75]Selenomethionine incorporation into human plasma proteins and erythrocytes.
    Jr. Metabolism, Clin. Exptl. 15:626-639, 1966.

14. Penner, J. A.: Seleno-methionine incorporation into hemoglobin.
    Clin. Res. 12:228, 1964.

15. VanGoidsenhoven, G. E., Denk, A. F., Pflezer, B. A., Knight, W. A.:
    Pancreatic metabolism of [75]Selenomethionine in dogs.
    Gastroenterology 33:403-411, 1967.

16. Zuidema, G. D. and Kirsch, M.: Pancreatic uptake of ^{75}Se-selenomethio-
    nine.
    Ann. Surg. 158:894-897, 1963.

17. Anghileri, L. J. and Marques, R. O.: Fate of injected selenium-75-
    tagged methionine and selenium-75-tagged cystine in mice.
    Arch. Biochem. Biophys. 111:580-582, 1965.

18. Awad, H. K., Potchen, E. J., Adelstein, J. and Dealy, J. B.: The
    regional distribution of [75]Selenomethionine in the rat.
    Metabolism 15:370-378, 1966.

19. Sternberg, J., Imbach, A.: Turnover studies with ^{75}Se-methionine in
    rats.
    Int. J. Appl. Rad. Isotopes 18:557-586, 1967.

20. Awad, H. K., Potchen, E. J., Adelstein, J. and Dealy, J. B.: The
    interconversion and reutilization of injected [75]Selenomethionine in
    the rat.
    J. Biol. Chem. 242:492-499, 1966.

21. Beierwaltes, W. H., Digiulio, W. and Sisson, J. C.: Parathyroid
    scanning. In "Scintillation Scanning in Clinical Medicine".
    Edited by J. L. Quinn, Philadelphia.
    W. B. Saunders Co., 1964, pp 55-68.

22. Bender, M. A. and Blau, M.: Pancreas scanning with Se[75]-L-seleno-
    methionine. In "Scintillation Scanning in Clinical Medicine".
    Edited by J. L. Quinn.
    Philadelphia, W. B. Saunders Co., 1964.

23. Blau, M., Manske, R. F., Bender, M.: Clinical experience with
    [75]Selenomethionine for pancreas visualization.
    J. Nucl. Med. 3:202, 1963.

24. Blau, M.: Pancreas scanning with Se[75]-selenomethionine.
    In "Medical Radioisotope Scanning".
    Vienna, International Atomic Energy Agency, 1964, vol. 2, pp 275-287.

25. King, E. R., Sharpe, A. and Greenberg, M.: A study of the morphology
    of the normal pancreas using Se[75]-methionine photoscanning.
    Am. J. Roentg. 96:657-663, 1966.

26. Sodee, D. B.: Radioisotope scanning of the pancreas with selenomethionine-Se[75].
    In "Medical Radioisotope Scanning".
    Vienna, International Atomic Energy Agency, 1964, vol. 2, pp 289-300.

27. Digiulio, W. and Beierwaltes, W. H.: Parathyroid scanning with selenium-75 labelled methionine.
    J. Nucl. Med. 5:417-427, 1964.

28. Sodee, D. B.: Radioisotope scanning of the pancreas with seleno-methionine (Se[75]).
    Radiology 83:910-916, 1964.

29. Blau, M. and Bender, M. A.: Se[75]-selenomethionine for visualization of the pancreas by isotope scanning.
    Radiology 78:974, 1962.

30. Sodee, D. B. et al: Dosimetry of selenomethionine-Se[75] for pancreatic scanning.
    Nucleonics 23(7):78-81, 1965.

31. Spencer, R. P. and Blau, M.: Intestinal transport of selenium-75 selenomethionine.
    Science N. Y. 136:155-156, 1962.

32. Hansson, E. and Blau, M.: Incorporation of selenomethionine-^{75}Se into pancreatic juice protein in vivo.
    Biochem. biophys. Res. Commun. 13:74.

33. Holland, J. F., Field, S., Bryant, B., Blau, M.: Sources and disposition of transplantable tumors.
    Proc. Amer. Soc. Cancer Res. 6:29, 1965.

34. Hansson, E. and Jacobsson, S. O.: Uptake of Se-selenomethionine in the tissues of the mouse studied by whole-body autoradiography.
    Biochem. biophys. Acta 115:285-293, 1966.

35. Blau, M. and Holland, J.: Metabolism of selenium-75 L-selenomethionine.
    In "Radioactive Pharmaceuticals".
    United States Atomic Energy Commission, April 1966, pp 423, 428.

36. Ochoa-Solano, A. and Gitler, C.: Incorporation of [75]Selenomethionine and ^{35}S-methionine into chicken egg white proteins.
    J. Nutrition 94:243-248, 1968.

37. Ochoa-Solano, A. and Gitler, C.: Digestion and absorption of ingested and secreted protein labeled with [75]Selenomethionine and ^{35}S-methionine in the GI tract of the rat.
    J. Nutr. 94:244-255, 1968.

38. Haynie, T. P., Svoboda, A. C. and Zuidema, G. D.: Diagnosis
    of pancreatic disease by photoscanning.
    J. Nucl. Med. 5:90-94, 1964.

39. Mlecko, L. M., Rodriguez, Antunez, A.: Scintigrams in the diagnosis
    of hepatic neoplasia.
    Am. J. Dig. Dis. 12:494-598, 1967.

40. Biagini, C., Colella, A. C. and Pigorini, F.: The visualization of
    the pancreas by means of scintigraphy (In Italian).
    Nunt. radiol., 29:935-939, 1963.

41. Nagai, T.: Preliminary studies with Se^{75}-methionine for clinical
    diagnosis of pancreas tumor.
    Radioisotopes, Tokyo 12:378-383, 1963.

42. Burke, G. and Goldstein, M. S.: Radioisotope photoscanning in the
    diagnosis of pancreatic disease.
    Am. J. Roentg. 92:1156-1161, 1964.

43. Rodriguez-Antunez, A.: Use of morphine in pancreatic scanning with
    Se^{75}-methionine.
    J. Nucl. Med. 5:729, 1964.

44. Rodriguez-Antunez, A.: Pancreatic scanning with selenium-75 methionine
    utilizing morphine to enhance contrast.
    Cleveland Clinic Quarterly 31:213-218, 1964.

45. Scheer, K. E. and Zum Winkel, K.: The use of a scintillation camera
    in clinical diagnostic studies.
    Minerva nucl. 9:386-390, 1965.

46. Aronsen, K. F., Gynning, I. and Walderskog, B.: Evaluation of
    ^{75}Se-selenomethionine for visualization of the pancreas by scanning
    technique.
    Acta chir. scand. 129:624-630, 1965.

47. Lahdevirta, J. and Haikonen, M.: Isotope scanning of the pancreas
    with ^{75}Se-methionine (In Finnish).
    Duodecim 81:1014-1023, 1965.

48. Laconi, A.: Research on pancreatic scintigraphy (In Italian).
    Minerva Med. 56:3645-3652, 1965.

49. Burdine, J. A. and Haynie, T. P.: Diagnosis of pancreatic carcinoma
    by photoscanning.
    J. Am. Med. Ass. 194:979-983, 1965.

50. Tabern, D. L., Kearney, J. and Dolbow, A.: The use of intravenous amino
    acids in the visualization of the pancreas with seleno-75-methionine.
    J. Nucl. Med. 6:762-766, 1965.

51. Potchen, E. J.: The thyroid uptake of selenium-75-selenomethionine. Effect of L-thyroxine and thyroid stimulating hormone. J. Nucl. Med. 7:433-441, 1966.

52. Sodee, D. B.: Pancreatic scanning. Radiology 87:641-645, 1966.

53. Van Vaerenbergh, M.: Pancreatography with radioisotopes (In French). Acta gastro-enter. belg. 29:197-210, 1966.

54. Potchen, E. J. and Sodee, D. B.: Selective isotopic labeling of the human parathyroid: a preliminary case report. J. Clin. Endocr. Metab. 24:1125-1128, 1964.

55. Haynie, T. P., Otte, W. K. and Wright, J. D.: Visualization of a hyperfunctioning parathyroid adenoma using Se[75]-selenomethionine and the photoscanner. J. Nucl. Med. 5:710-714, 1964.

56. Potchen, E. J. et al: Radioisotopic localization of the overactive human parathyroid. Am. J. Roentg. 93:955-961, 1965.

57. Sack, H., Petry, R. and Duwell, H. J.: The demonstration of an adenoma of the parathyroids by ^{75}Se-methionine and the scintillation camera. Dt. med. Wschr. 90:2353-2354, 1965.

58. Potchen, E. J., Wilson, R. E. and Dealy, J. B.: External parathyroid scanning with Se[75]-selenomethionine. Ann. Surg. 162:492-504, 1965.

59. Gottschalk, A.: Bilateral intra-arterial injection in the thyrocervical trunk. A technique to facilitate localization of parathyroid adenomas with selenium-75 methionine. J. Nucl. Med. 7:374-375, 1966.

60. Bartelheimer, H. and Fritzsche, H.: The discovery of an adenoma of the parathyroids by scintigraphy with selenium-75 methionine (In German). Klin. Wschr. 43:854-856, 1965.

61. Marshall, R. B., Roberts, D. K. and Turner, R. A.: Adenomas of the parathyroid gland. Cancer 20:512-524, 1967.

62. Herrera, N. E., Gonzalez, R., Belski, J.: ^{75}Se-methionine as a diagnostic agent in malignant lymphoma. J. Nucl. Med. 6:792-804, 1965.

63. Spencer, R., Montana, G., Evans, O. R.: Uptake of Selenomethionine by mouse and in human lymphomas.
    J. Nucl. Med. 8:117-208, 1967.

64. Potchen, E. J.: Isotopic labeling of the rat parathyroid as demonstrated by autoradiography.
    J. Nucl. Med. 4:480-484, 1963.

65. Shimazu, F. and Tappel, A. L.: Selenoamino acids as radiation protectors in vitro.
    Radiat. Res. 23:210-217, 1964.

66. Shimazu, F. and Tappel, A. L.: Selenoamino acids: decrease of radiation damage to amino acids and proteins.
    Science, N. Y. 143:369-371, 1964.

67. Cassen, B., Curtis, L., Reed, C. and Libby, R.: Instrumentation of ^{131}I use in medical studies.
    Nucleonics 9(2):46-50, 1951.

68. Newell, R. R., Saunders, W., Miller, E.: Multichannel collimators for gamma-ray scanning with scintillator counters.
    Nucleonics 10(7):36-40, 1952.

69. Allen, H. C., Risser, R. J., Green, J. A.: Improvements in outlining of thyroid and localization of brain tumors by the application of sodium iodide gamm-ray spectrometry techniques.
    Proc. 2nd Oxford Radioisotope Conference, vol. 1, pp 76-96, Academic Press, New York, 1954.

70. Mayneord, W. V. and Newberg, S. P.: An automatic method of studying the distribution of activity in a source of ionizing radiation.
    Brit. J. Radiol. N. S. 25:584-586, 1952.

71. Kuhl, D. E., Chamberlain, R. H., Hale, J., Gorson, R. O.: A high-contrast photographic recorder for scintillation counter scanning.
    Radiology 66:730-739, 1956.

72. Mallard, J. R. and Peachey, C. J.: A quantitative automatic body scanner for the localization of radioisotopes in vivo.
    Brit. J. Radiol. 32:652-657, 1959.

73. Medical Radioisotope Scanning, vols. 1, 2.
    International Atomic Energy Agency, Vienna 1965.

74. Radioactive Pharmaceuticals.
    U. S. Atomic Energy Commission, CONF-651111, 1966.

75. Schlundt, H., Barker, H. H., Flinn, F. B.: Determination and Estimation of Radium and Mesothorium in Living Persons.
    Amer. J. Roentgenol. 21:345-348, 1929.

76. Reines, F., Schuch, R. L., Anderson, E. L.: Determination of total body radioactivity using liquid scintillation detectors. Nature (Lond.) 172:521-523, 1953.

77. Marinelli, L. D., Miller, E. E., Gustafson, P. S.: Determination of gamm-ray emitting isotopes in living persons. Amer. J. Roentgenol. 73:661-671, 1955.

78. Miller, C. E.: Low Intensity Spectrometry of the Gamma Radiation Emitted by Human Beings. Proc. 2nd UN Int. Conf. PUAE 23:113-123, 1958.

79. May, H. A., Marinelli, L. D.: Sodium Iodide Systems in Whole-Body Counting. IAEA, pp 16-36, Vienna, 1962.

80. Miller, C. E.: An Experimental Evaluation of Crystal Techniques. IBID, pp 82-120.

81. Rundo, J.: Some Calibration Problems of Whole-Body Gamma-Ray Spectrometers. IBID, pp 121-137.

82. Carr, E. A., Jr.: The development of myocardial scanning with special reference to the use of ^{131}Cs. In "Scintillation Scanning in Clinical Medicine". J. L. Quinn, III W. B. Saunders, Co., Philadelphia, 1964, pp 93-103.

83. Carr, E. A., Jr., Beierwaltes, W. H., Wegst, A. V. and Bartlett, J. D.: Myocardial scanning with ^{86}Rb. J. Nucl. Med. 3:76, 1962.

84. Loevinger, R., Jopha, E. M. and Brownell, G. L.: Discrete radio-isotope sources. In "Radiation Dosimetry". Hine , G. J. and Brownell, G. L. (Eds.) Academic Press, New York, 1956, pp 693-728.

85. Sintex, F. M., McMullen, J., Hastings, A. B.: The effect of insulin on the incorporation of ^{14}C into the protein of rat diaphragm. J. Biol. Chem. 198:615-619, 1952.

86. Krahl, M. E.: Incorporation of ^{14}C-amino acids into glutothione and protein fractions of normal and diabetic rat tissues. J. Biol. Chem. 200:99-109, 1953.

87. Manchester, K. L. and Young, F. G.: The effect on insulin on incorporation of amino acids into protein of normal rat diaphragms "in vivo". Biochem. J. 70:353-358, 1958.

88. Wang, C. C. and Robbins, L. L.: Biological and Medical Effects of Radiation.
    In "Radiation Dosimetry". Hine, G. J. and Brownell, G. L. (Eds.) Academic Press, New York, 1956, pp 125-152.

89. Seltzer, R. A., Kereianes, J. G. and Saenger, E. L.: Radiation exposure from radioisotopes in pediatrics.
    New England J. Med. 271:84-99, 1964.

90. Burke, G. and Goldstein, M. S.: Radioisotope photoscanning in the diagnosis of pancreatic disease.
    Amer. J. Roentgen. 92:1156-1161, 1964.

91. Haynie, T. P., Svoboda, A. C. and Zuidema, G. D.: Diagnosis of pancreatic disease by photoscanning.
    J. Nucl. Med. 5:90-94, 1964.

92. Sodee, D. B.: Diagnostic photoscanning of the pancreas.
    Ann. Intern. Med. 60:722, 1964.

93. Burdine, J. A. and Haynie, T. P.: Diagnosis of pancreatic carcinoma by photoscanning.
    J.A.M.A. 194:979-983, 1965.

94. Eaton, S. B., Potsaid, M. S., Lo, H. H. and Beaudien, E.: Radioisotopic "Subtraction" scanning for pancreatic lesions.
    Radiology 89:1033-1039, 1967.

95. Thomas, J. E.: Mechanism of action of pancreatic stimuli studied by means of atropine-like drugs.
    Am. J. Physiol. 203:124-128, 1964.

96. Sangster, A. J.: The uses of morphine and propantheline in intravenous cholecystography.
    Lancet 2:525-527, 1955.

APPROVAL SHEET

The dissertation submitted by Moshe Ben-Porath has been read and approved by five members of the faculty of the Graduate School of Loyola University.

The final copies have been examined by the director of the dissertation and the signature which appears below verifies the fact that any necessary changes have been incorporated, and that the thesis is now given final approval with reference to content, form and mechanical accuracy.

The dissertation is therefore accepted in partial fulfillment of the requirements for the Degree of Doctor of Philosophy.

Date

Signature of Advisor